

---

Masters Theses

Student Theses and Dissertations

---

Summer 2011

## Quantitative oxygen imaging with a display screen and a color camera

Sanghan Park

Follow this and additional works at: [https://scholarsmine.mst.edu/masters\\_theses](https://scholarsmine.mst.edu/masters_theses)



Part of the [Electrical and Computer Engineering Commons](#)

Department:

---

### Recommended Citation

Park, Sanghan, "Quantitative oxygen imaging with a display screen and a color camera" (2011). *Masters Theses*. 4502.

[https://scholarsmine.mst.edu/masters\\_theses/4502](https://scholarsmine.mst.edu/masters_theses/4502)

This thesis is brought to you by Scholars' Mine, a service of the Missouri S&T Library and Learning Resources. This work is protected by U. S. Copyright Law. Unauthorized use including reproduction for redistribution requires the permission of the copyright holder. For more information, please contact [scholarsmine@mst.edu](mailto:scholarsmine@mst.edu).

QUANTITATIVE OXYGEN IMAGING WITH A DISPLAY SCREEN AND A  
COLOR CAMERA

by

SANGHAN PARK

A THESIS

Presented to the Faculty of the Graduate School of the  
MISSOURI UNIVERSITY OF SCIENCE AND TECHNOLOGY

In Partial Fulfillment of the Requirements for the Degree  
MASTER OF SCIENCE IN ELECTRICAL ENGINEERING

2011

Approved by

Dr. Chang-Soo Kim

Dr. Randy H. Moss

Dr. Minsu Choi

© 2011  
Sanghan Park  
All Rights Reserved

## **PUBLICATION THESIS OPTION**

This thesis consists of the following two articles:

Paper 1: pages 9 - 25 will be presented as a conference proceeding in the SPIE Defense,

Security and Sensing to be held at Orlando, FL, USA on April 28th, 2011.

Paper 2: pages 26 - 48 will be submitted to Sensors and Actuators B - Chemical.

## ABSTRACT

Optical oxygen sensing uses luminophores such as metal complex dyes that respond to oxygen when illuminated by their specific excitation wavelengths. Traditional optical instruments are mostly spectrometric instruments based on the measurements of emission, absorption or reflection. There is, however, a great need to develop simple, economical, photometric detection components toward quantitative and two-dimensional imaging instruments.

In this work, familiar optoelectronic devices were utilized to demonstrate a simple determination method of gaseous oxygen both quantitatively and qualitatively. A liquid crystal display (LCD) screen and a color charge-coupled device (CCD) camera were employed as a light source for fluorescence excitation and a photodetector for emission measurement, respectively. Meso-scale test platforms incorporating fluidic channels and oxygen sensor films were prepared. The ruthenium-complex sensor films were excited by blue light displayed from the LCD screen to emit fluorescence responding to gaseous oxygen. The color camera was used successfully to characterize red fluorescence emission from sensor films based on colorimetric intensity measurements.

This method has an advantage over simplicity of the equipment and is considered a good alternative approach to time-resolved methods for relatively short-term monitoring. This combination of LCD and color camera enables a capability of uniform illumination over a large area with variable wavelength ranges to image spatial distribution of chemicals and to analyze multiple target analytes simultaneously.

## ACKNOWLEDGMENTS

The work in this thesis has been solely possible with the support and guidance of my advisor, Dr. Chang-Soo Kim. I wish to express my sincere thanks to Dr. Kim for his time deliberating on challenges, devising solutions, and his constant encouragement throughout this study. His direction has been invaluable and will be forever appreciated.

I also wish to express my sincere thanks to Dr. Randy Moss for his amazing lectures to foster overall knowledge related with image processing techniques. I am indebted to Dr. Minsu Choi for his suggestions in designing my analysis programs, and pointers for my defense.

My recommenders, Dr. Myeungho Oh, Air Force Col. Woongwoo Nam, and Army LC. Jaegu Kim, permitted me to use their names as references when I applied to this institution.

I want to give a special thank to my fellow lab mates Satya Gowthami, and Dr. Jongwon Park for their limitless support and encouragement.

I wish to express my endless gratitude to my family: especially to my father Youngwon Park, mother Deuksun Lee, and my wife Insun Lee for their immense patience, moral support and encouragement.

Appreciation is also extended to my sponsor Republic of Korea Army Headquarter.

## TABLE OF CONTENTS

	Page
PUBLICATION DISSERTATION OPTION.....	iii
ABSTRACT.....	iv
ACKNOWLEDGMENTS.....	v
LIST OF ILLUSTRATIONS.....	ix
LIST OF TABLES.....	xi
<b>SECTION</b>	
1. INTRODUCTION.....	1
1.1 OXYGEN SENSING.....	1
1.2 OPTICAL OXYGEN IMAGING TECHNIQUES.....	2
1.2.1. Optical Oxygen Sensing.....	2
1.2.2. Absolute Intensity Imaging.....	4
1.2.3. Time-resolved Imaging.....	4
1.3 MAJOR COMPONENTS OF THIS RESEARCH.....	5
1.3.1. Excitation Light Source.....	5
1.3.2. Photodetector.....	5
1.3.3. Luminophore.....	6
REFERENCES .....	7
<b>PAPER</b>	
I. FLUORESCENCE INTENSITY MEASUREMENTS WITH DISPLAY SCREEN AS EXCITATION SOURCE.....	9
ABSTRACT.....	9
Keywords.....	9
1. INTRODUCTION.....	10
2. EXPERIMENTS.....	12
2.1 MATERIALS AND EQUIPMENT.....	12
2.1.1. Optical Oxygen Sensor.....	12
2.1.2. Excitation Light Source.....	12
2.1.3. Photodetector.....	12
2.1.4. Long Pass Filter.....	14

2.2. FLUIDIC DEVICE PREPARATION.....	14
2.3. MEASUREMENT SETUP.....	15
2.4. EXPERIMENTAL PROCEDURE AND ANALYSIS METHOD.....	17
3. RESULTS AND DISCUSSION.....	18
3.1. SPECTRAL ANALYSIS OF OXYGEN PATCH SENSITIVITY AND LCD EMISSION.....	18
3.2. SENSOR IMAGE ANALYSIS.....	19
3.3. OXYGEN SENSITIVITY.....	20
4. CONCLUSION.....	23
REFERENCES.....	24
II. QUANTITATIVE OXYGEN IMAGING WITH A DISPLAY SCREEN AND A COLOR CAMERA.....	26
ABSTRACT.....	26
Keywords.....	26
1. INTRODUCTION.....	27
2. EXPERIMENTS.....	30
2.1. MATERIALS AND EQUIPMENT.....	30
2.1.1. Oxygen Sensor Coating.....	30
2.1.2. Sensor Platform.....	31
2.1.3. Liquid Crystal Display.....	32
2.1.4. Color Camera.....	33
2.2. CHARACTERIZATION.....	34
2.2.1. Measurement Procedure.....	34
2.2.2. Image Analysis Procedure.....	35
3. RESULTS AND DISCUSSION.....	37
3.1 OXYGEN SENSOR PATCH ANALYSIS.....	37
3.2 RECTANGULAR SENSOR PLATFORM.....	39
3.3 Y-JUNCTION SENSOR PLATFORM.....	41
4. CONCLUSION.....	46
REFERENCES.....	47

SECTION

2. CONCLUSION.....49

APPENDICES

A. DETAILED PROCEDURE FOR OXYGEN SENSOR COCKTAIL.....50

B. SENSOR PLATFORM PREPERATION.....52

C. MATLAB CODE FOR ANALYSIS.....55

VITA.....68

## LIST OF ILLUSTRATIONS

Figure	Page
<b>SECTION</b>	
1.1. Principle of luminescence quenching by molecular oxygen ( $\lambda_{ex}$ : excitation wavelength, $\lambda_{em}$ : emission wavelength).....	2
<b>PAPER I</b>	
1. Sensor platform and measurement setup.....	15
2. Photograph of the setup.....	16
3. Spectra of a commercial oxygen sensor patch (RedEye™) taken at various ratios of gaseous oxygen obtained with a spectrometer.....	18
4. Spectra of three primary colors (blue, green and red) displayed by an LCD monitor.....	19
5. Cropped ROI images (about 3 mm x 3 mm) at different gaseous oxygen percentages and their histograms.....	20
6. Variation in the red color intensity of ten images taken at a time at different oxygen percentages.....	22
7. Stern-Volmer plot of the red intensity of digital images versus gaseous oxygen percentage (n=3).....	22
<b>PAPER II</b>	
1. Two types of meso-scale, gas fluidic sensor platforms (not in real scale).....	32
2. A color camera takes pictures of the fluidic sensor platform installed in close proximity to an LCD screen that provides an excitation light with uniform intensity over the sensor coating.....	35
3. Spectra of three primary colors (blue, green and red) displayed by an LCD screen.....	37
4. Stern-Volmer plot of the red intensity of a commercial oxygen sensor patch (RedEye™) versus gaseous oxygen percentage (n=4).....	38

- 5. Visualization of oxygen distribution over the rectangular sensor area as defined in Fig. 1.....40
- 6. Images of Y-junction sensor and calibration curves for quantitative analysis.....43
- 7. Vertical profiles of various parameters across the Y-junction main channel at three locations of V1, V2 and V3 defined in Fig. 1(b).....44

**LIST OF TABLES**

Table	Page
PAPER I	
1. CCD camera setting conditions to acquire digital images of oxygen sensor patches.....	13
PAPER II	
1. Optimized CCD camera setting conditions used for this study.....	34

## **SECTION**

### **1. INTRODUCTION**

Familiar optoelectronic devices were utilized to demonstrate a simple, quantitative determination method of gaseous oxygen. A liquid crystal display (LCD) monitor was used as an excitation light source in this research. A color charge-coupled device (CCD) camera was employed as a photodetector to image luminescence intensities of sensor films with respect to oxygen. Meso-scale device platforms incorporating fluidic channels and ruthenium-complex oxygen sensors were prepared and its performance was characterized based on colorimetric absolute intensity measurements.

#### **1.1 OXYGEN SENSING**

Oxygen sensing is one of the most common, frequently required issues in life sciences, environment and many other industrial areas. Biologically, oxygen comprises most of the mass of living organisms such as proteins, carbohydrates and fats. Therefore, oxygen is related to many metabolic functions in most of the live beings.

Environmentally, oxygen sensing is essential for investigating water contamination in limnology and oceanography.

There are two major categories of oxygen sensing methods. The first category is the electrochemical determination utilizing amperometric or galvanic electrodes. The second one is based on optical methods where majority of them utilize fluorophores that respond to oxygen. Optical oxygen sensors are becoming dominant over electrochemical types. This non-destructive sensing mechanism does not consume oxygen, hence there is

no perturbation of oxygen environment during the use of sensor. Other advantages include its potential for easier device miniaturization with simple structure, the capability of remote sensing with non-invasive and non-contact nature and the compatibility with two-dimensional imaging of oxygen distribution.

## 1.2 OPTICAL OXYGEN IMAGING TECHNIQUES

**1.2.1. Optical Oxygen Sensing.** Optical oxygen sensors use the mechanism of oxygen quenching as shown in Fig.1.1. Quenching is a phenomenon of emission intensity decrease of a luminophore in presence of a quencher.

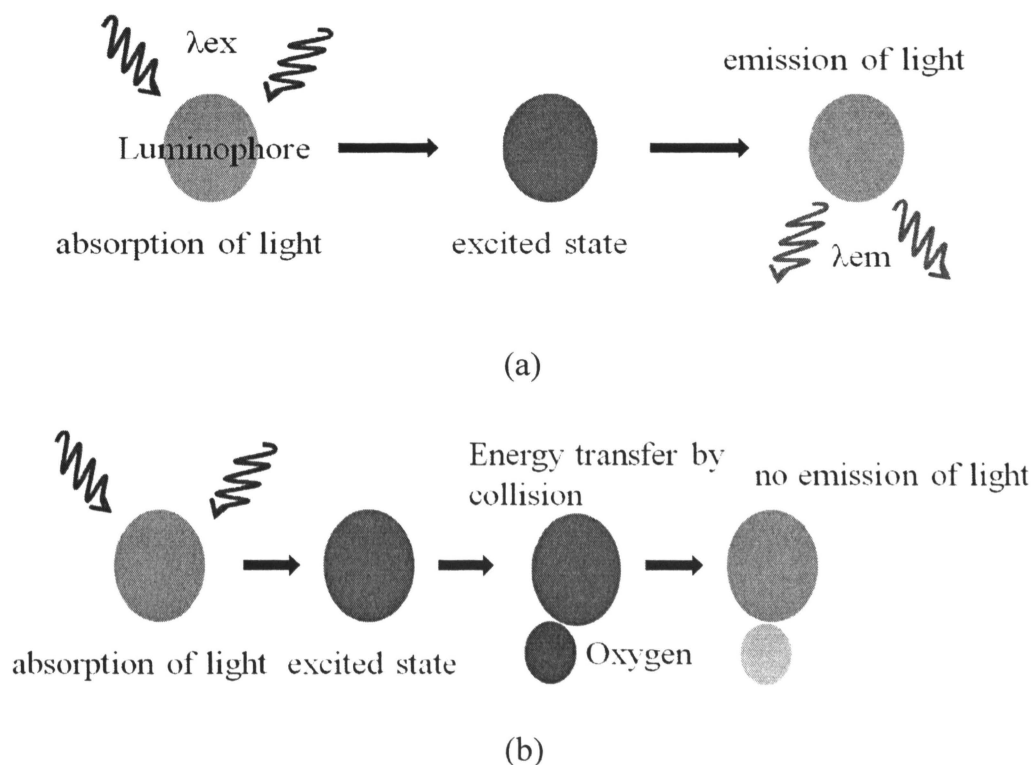


Figure 1.1. Principle of luminescence quenching by molecular oxygen ( $\lambda_{ex}$ : excitation wavelength,  $\lambda_{em}$ : emission wavelength) (a) Luminescence process in the absence of oxygen, (b) Deactivation of the luminescent indicator molecule by molecular oxygen

In this case, oxygen molecule acts as a powerful quencher of the electronically excited state of the luminophore. Oxygen sensitive luminophores immobilized within an oxygen permeable matrix emit light with its characteristic wavelength when illuminated by a light source with adequate excitation wavelength range. These luminophores include metal-complex organic dyes, dual emitters and fullerenes [1]. Many recent studies use ruthenium- and porphyrin-complexes as luminophores [2-4].

Oxygen concentration can be determined from optical oxygen sensors by measuring intensity, lifetime or phase shift based on the Stern-Volmer relationship as follows [5]:

$$I_0/I (= \tau_0/\tau = \Phi_0/\Phi) = 1 + K_{SV} [O_2] \quad (1)$$

where  $I_0$  and  $I(\tau, \Phi)$  represent the steady-state luminescence intensities without and with the quencher (here oxygen). Alternately,  $\tau$  and  $\Phi$  represent the lifetime (decay time) of luminescence when a constant excitation light is switched off and the phase angle shift of luminescence (time delay) from a sinusoidal excitation light caused by its decay lifetime, respectively.  $K_{SV}$  is the Stern-Volmer quenching constant and  $[O_2]$  is the oxygen concentration, respectively. Therefore, the ratio of luminescence intensities without and with oxygen ( $I_0/I$ ) becomes linearly proportional to the oxygen concentration.

**1.2.2. Absolute Intensity Imaging.** The most straight forward, simple method of two-dimensional oxygen mapping is to record the image of absolute luminescence intensity over a planar sensor film in contact with the sample environment. Mostly, low-noise monochromatic charge-coupled device (CCD) cameras are used for this purpose with appropriate optical filters to selectively accept the luminescence wavelength. It is generally known that the absolute intensity tends to drift over time due to the photobleaching or leaching of the oxygen-sensitive luminophores and fluctuation of excitation light source intensity. The intensity method, however, has an advantage over simplicity of the equipment, thus still is a good option for relatively short-term monitoring.

**1.2.3. Time-resolved Imaging.** To circumvent this instability issue of intensity measurements, two different time-resolved techniques were developed which include the luminescence lifetime imaging and phase shift imaging. As shown in Eq. (1), theoretically the ratios of lifetime ( $\tau_0/\tau$ ) and phase shift ( $\Phi_0/\Phi$ ) are also linearly proportional to oxygen concentration. The lifetime or phase shift imaging method records the two-dimensional distributions of the decay time or phase shift of luminescence responding to their respective excitation source. Then, an image of the lifetime or the phase shift distribution is reconstructed for visualization over an area to be analyzed. Therefore, special excitation light sources operated by pulse and sinusoidal waves and synchronized high-speed cameras are required for these time-resolved methods.

## 1.3 MAJOR COMPONENTS OF THIS RESEARCH

**1.3.1. Excitation Light Source.** The common way of exciting a luminophore for emission is done by using light-emitting diode (LED) bulbs or broad-band sources with filters. In this study, an LCD monitor (HP 2159m, 21.5" color LCD monitor, Hewlett-Packard) was used as the excitation light source. A commercial LCD monitor mixes three primary color wavelengths (red, green and blue) to display true color (i.e. 16,777,216 different colors with 24-bit RGB color space). Several new techniques are recently emerging where these devices are applied for chemical quantification purposes. Especially, Filippini et al. implemented the idea of computer screen photo-assisted technique (CSPT) where commercial LCD monitors were used as illumination light source for analytical applications [6-12]. These examples include illuminating samples for transmission/absorption measurements and exciting luminescent samples for emission measurements.

**1.3.2. Photodetector.** Spectrometer is the most common device used for measuring the luminescence quenching by oxygen through absolute intensity, phase shift or lifetime measurements. A different approach was made in this study that uses a common CCD color camera as the photometric data acquisition device. Several recent studies on oxygen determination based on color images were reported [3,4,13]. It was demonstrated that the digital color camera was very useful as a photometric equipment for quantitative oxygen determination because the spectral sensitivity of the red pixel matched well with the emission wavelength of the oxygen-responsive luminophores. This familiar device can provide significant advantages to store data digitally with two-

dimensional information and analyze its color change and gradient over a captured image area. A digital single-lens reflex (DSLR) camera ( $\alpha$ 350 DSLR camera, 14.2 Megapixel, Sony) was used in this study.

**1.3.3. Luminophore.** In this study, ruthenium complex, dichlorotris (1,10-phenanthroline) ruthenium (II) hydrate was used as the oxygen sensing fluorophore. When ruthenium complex is excited at its excitation wavelength (about 470 nm peak), it emits light at its emission wavelength (about 590 nm peak). In presence of a quenching molecule (here oxygen), however, excess energy is transferred to the oxygen molecule non-radiatively to quench the fluorescence intensity. Therefore, the intensity of emission decreases with increasing oxygen concentration. A commercially available ruthenium based oxygen sensor patch (RedEye<sup>TM</sup>, RE-FOX-8, 8 mm diameter, OceanOptics) was first used for a proof-of-concept demonstration. This oxygen sensor patch has ruthenium-complex sensor formulation immobilized within a sol-gel matrix. Later, meso-scale planar sensor films formulated in our laboratory were used for oxygen imaging. This was prepared by mixing ruthenium complex with silicone matrix and spin-coating on glass plates.

## REFERENCES

- [1] X-d. Wang, H-x. Chen, Y. Zhao, X. Chen, X-r. Wang, "Optical oxygen sensors move towards colorimetric determination," *Trends in Analytical Chemistry*, 29 (4), 319-338, 2010
- [2] Eun Jeong Cho, Frank V. Bright, "Integrated chemical sensor array platform based on a light emitting diode, xerogel-derived sensor elements, and high-speed pin printing," *Analytica Chimica Acta*, 470, 101-110, 2002
- [3] Gerhard Holst, Bjorn Grunwald, "Luminescence lifetime imaging with transparent oxygen optodes," *Sensors and Actuators B*, 74, 78-90, 2001
- [4] Paul Hartman, Werner Ziegler, Gerhard Holst, Dietrich W. Lubbers, "Oxygen flux fluorescence lifetime imaging," *Sensors and Actuators B*, 38-39, 110-115, 1997
- [5] E.R. Carraway, J.N. Demas, B.A. DeGraff, J.R. Bacon, "Photophysics and photochemistry of oxygen sensors based on luminescent transition metal complexes," *Anal. Chem.* 63, 337-342, 1991
- [6] J. Manzano, D. Filippini, and I. Lundström, "Computer Screen Illumination for the Characterization of Colorimetric Assays," *Sensors and Actuators B - Chemical*, 96 (1-2), 173-179, 2003
- [7] D. Filippini, G. Comina, and I. Lundström, "Computer Screen Photo-Assisted Reflectance Fingerprinting," *Sensors and Actuators B - Chemical*, 107 (2), 580-586, 2005
- [8] D. Filippini, J. Bakker, and I. Lundström, "Fingerprinting of Fluorescent Substances for Diagnostic Purposes using Computer Screen Illumination," *Sensors and Actuators B - Chemical*, 106 (1), 302-310, 2005
- [9] D. Filippini, and I. Lundström, "Preferential Color Substances and Optimized Illuminations for Computer Screen Photo-Assisted Classification," *Analytica Chimica Acta*, 557 (1-2), 393-398, 2006
- [10] S. Macken, I. Lundström, and D. Filippini, "Optical Properties of Microstructures for Computer Screen Photoassisted Experiments," *Applied Physics Letters*, 89 (25), 254104, 2006

- [11] E. Gatto, M. A. Malik, C. D. Natale, R. Paolesse, A. D'Amico, I. Lundstrom, D. Filippini, "Polychromatic Fingerprinting of Excitation Emission Matrices," *Chemistry - A European Journal* 14 (20), 6057-6060, 2008
- [12] M. A. Malik, E. Gatto, M. A. Malik, S. Macken, C. DiNatale, R. Paolesse, A. D'Amico, I. Lundstrom, D. Filippini, "Imaging Fingerprinting of Excitation Emission Matrices," *Analytica Chimica Acta*, 635 (2), 196-201, 2009
- [13] Gregor Liebsch, Ingo Klimant, Bernhard Frank, Gerhard Holst, Otto S. Wolfbeis, "Luminescence lifetime imaging of oxygen, pH, and carbon dioxide distribution using optical sensors," *Applied spectroscopy*, 54(4), 549-559, 2000

## **PAPER**

### **I. FLUORESCENCE INTENSITY MEASUREMENTS WITH DISPLAY SCREEN AS EXCITATION SOURCE**

#### **ABSTRACT**

Several new techniques are emerging to use digital display devices as a new type of light source for analytical purposes. We demonstrate the use of a liquid crystal display (LCD) computer screen as an excitation light source for determining gaseous oxygen contents over a relatively large area. Meso-scale device platforms are prepared with glass plates incorporating fluidic channels and commercial oxygen sensor patches. Fluorophores are excited by the blue wavelength range from the LCD computer screen. The sensor signals exhibit a good linear relationship with respect to the oxygen content. The display devices, with a capability of uniform illumination over a large area for variable wavelengths, have a great potential as a light source for high-throughput, multiple-analyte, quantitative chemical analysis.

#### **Keywords**

optical oxygen sensor, liquid crystal display (LCD), color camera, charge-coupled device (CCD), colorimetry

## 1. INTRODUCTION

Molecular oxygen is one of the major species for the metabolism of organisms and also for a majority of biochemical processes. Consequently, there are many application fields where oxygen determination is critical. The most common sensing moiety has been the electrochemical method such as using Clark type or galvanic type oxygen sensors. Optical oxygen sensing, however, is now becoming the main trend to replace those electrochemical sensors. This is based on luminescence quenching that does not require consumption of oxygen. Oxygen is a very powerful quencher, thus some oxygen-responsive luminescent molecules get quenched in the presence of oxygen. These luminophores include metal-complex organic dyes, dual emitters and fullerenes [1]. Many recent studies use ruthenium- and porphyrin-complexes as sensing probes. These materials emit oxygen-responsive light of a specific wavelength range when excited at shorter wavelength of lights. Either the intensity, emission decay time or phase-shift measurements can be used to determine oxygen quantitatively in terms of concentration or pressure.

Rapid technological progress in digital display devices, such as LCD (liquid crystal display), LED (light-emitting diode), OLED (organic light-emitting diode) and DLP (digital light projectors) make these optoelectronic products nearly ubiquitous around our daily lives. Commercial LCD monitors can display over 16 million colors by mixing red, green and blue (RGB) elemental wavelength ranges. Several new techniques are recently emerging where these devices are applied to chemical quantification purposes. Especially, Filippini et al. implemented the idea of computer screen photo-assisted technique (CSPT) where commercial LCD monitors were used as illumination

light sources for analytical applications [2-8]. These examples include illuminating samples for transmission/absorption measurements and exciting luminescent samples for emission measurements.

In this work, adopted this technique to use an LCD computer screen as an excitation light source for determining gaseous oxygen contents. As a proof-of-concept model system, meso-scale device platforms are prepared with glass plates incorporating fluidic channels and commercial oxygen sensor patches. Fluorophores immobilized in the sensor patch are excited by the blue wavelength range (about 470 nm peak) from the LCD computer screen. The fluorescence intensity was measured with respect to gaseous oxygen contents by a simple photometric method. Digital images of the sensor patch were acquired with a charge-coupled device (CCD) color camera and their red pixel intensities were analyzed [9-11].

## 2. EXPERIMENTS

### 2.1 MATERIALS AND EQUIPMENT

**2.1.1 Optical Oxygen Sensor.** In this study, ruthenium complex is used as an oxygen sensing material. The basic principle behind oxygen sensing is luminescence quenching where the oxygen molecule acts as a quencher. When ruthenium complex is excited at its excitation wavelength (about 470 nm peak), it emits light at its emission wavelength (about 590 nm peak). In the presence of a quenching molecule (here oxygen), however, excess energy is transferred to the oxygen molecule non-radiatively to quench the fluorescence emission. Therefore, the intensity of fluorescence emission decreases with increasing oxygen concentration. We used a commercially available ruthenium based oxygen sensor patch (RedEye™, RE-FOX-8, 8 mm diameter, OceanOptics) to conduct quantitative oxygen concentration measurements. This oxygen sensor patch has ruthenium-complex sensor formulation immobilized within a sol-gel matrix.

**2.1.2 Excitation Light Source.** The common way of exciting a fluorophore at its excitation wavelength is done by using LED bulbs or broad-band sources with filters. In this study, an LCD monitor (HP 2159m, 21.5" color LCD monitor, Hewlett-Packard) was used as the excitation light source. A commercial LCD monitor mixes three major color wavelengths (red, green and blue) to display true color (i.e. 16,777,216 different colors with 24-bit RGB color space).

**2.1.3 Photodetector.** A spectrofluorometer is the most common device used for measuring the fluorescence quenching by oxygen through either absolute intensity, phase

shift or lifetime measurements. We used a different approach instead that uses a common CCD camera as a photometric data acquisition device. This familiar device can provide significant advantages to store data digitally with two-dimensional information and analyze its color change and gradient over a captured image area. A digital single-lens reflex (DSLR) camera ( $\alpha$ 350 DSLR camera, 14.2 Megapixel, Sony) was used in this study. The camera was operated in Manual Mode to manually select the camera settings and to prevent automatic image correction by the camera. Various camera setting conditions for this study are shown in Table. 1. The optimum setting values were selected from our repeated experiments and may be combined in different ways depending on the experimental conditions.

Table 1. CCD camera setting conditions to acquire digital images of oxygen sensor patches.

<b>Parameters</b>	<b>ISO</b>	<b>Shutter speed</b>	<b>White balance</b>	<b>F number</b>	<b>Focus</b>
<b>Setting values</b>	400	0.8"	Sunlight	5.6	Slightly unfocused

**2.1.4 Long Pass Filter.** The spectral sensitivity of built-in Bayer color filters on the image sensor chip of a commercial camera product is usually proprietary information not available from manufacturers. Although very limited, it is generally known that the red pixel has sensitivity over the blue and green wavelength ranges as well. Therefore, an optical long pass filter (OG550, cut-off wavelength 550 nm, square 2"x2", Thorlabs) was employed in our study to remove the background blue wavelength because of the strong excitation light source compared with the emission light intensity of the sensor. This filter may also further minimize the noise level caused by unexpected short wavelength light.

## **2.2 FLUIDIC DEVICE PREPARATION**

A simple meso-scale fluidic sensor platform was prepared. As shown in Fig. 1 (a), it consists of two glass plates, two glass spacers and 1/8" polyethylene tubing. The fluidic channel is formed between the two glass plates (area 75mm x 50mm x 1mm) utilizing the glass spacers (75mm x 25mm x 3mm) as channel walls, thus creating a meso-scale channel 75mm long, 10mm wide and 3mm high. All components were glued with an epoxy. The polyethylene tubing (inner diameter 1/8") is used as gas inlet and outlet ports. The optical oxygen sensor patch was placed within the channel.

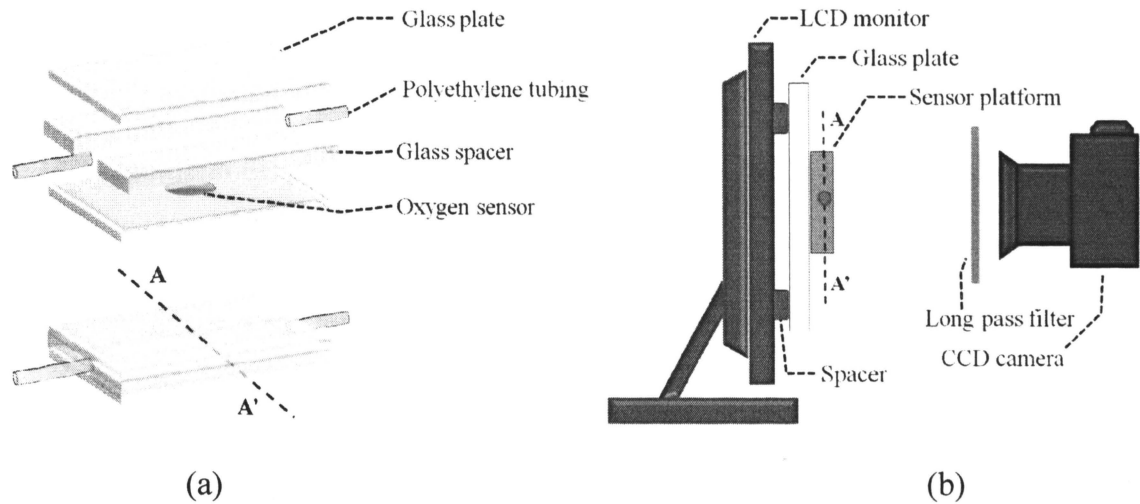


Fig. 1. Sensor platform and measurement setup (a) Structure of the meso-scale fluidic sensor platform: before assembly (top) and after assembly (bottom). (b) Measurement setup with an LCD monitor as excitation light source and a color camera as photodetector.

### 2.3 MEASUREMENT SETUP

The test setup is as shown in Fig. 1 (b). A glass plate (1.5 mm thick) was sandwiched between the fluidic sensor platform and the surface of the LCD monitor using elastic spacers (5 mm thick) to minimize any thermal radiation from the monitor. This was to eliminate thermal fluctuation of the optical oxygen sensor. The sensor platform was located on the glass plate surface. A long pass filter was placed in front of the camera lens to remove the excessive blue light. The whole setup was placed in a darkroom to minimize the interference of stray light.

A spectral analysis was conducted with a traditional spectrometer (USB2000-FLG, OceanOptics) to characterize the oxygen patch sensitivity and the three elemental colors from LCD monitor. As shown in Fig. 2, a reflection probe (R400-7-UV-VIS, OceanOptics) was brought in close proximity to the surface of the fluidic sensor platform to excite the sensor patch with an LED bulb (LS450, peak 470 nm, Ocean Optics) and measure the oxygen-responsive emission. Also, the same reflection probe was used to bring the LCD emission to the spectrometer.

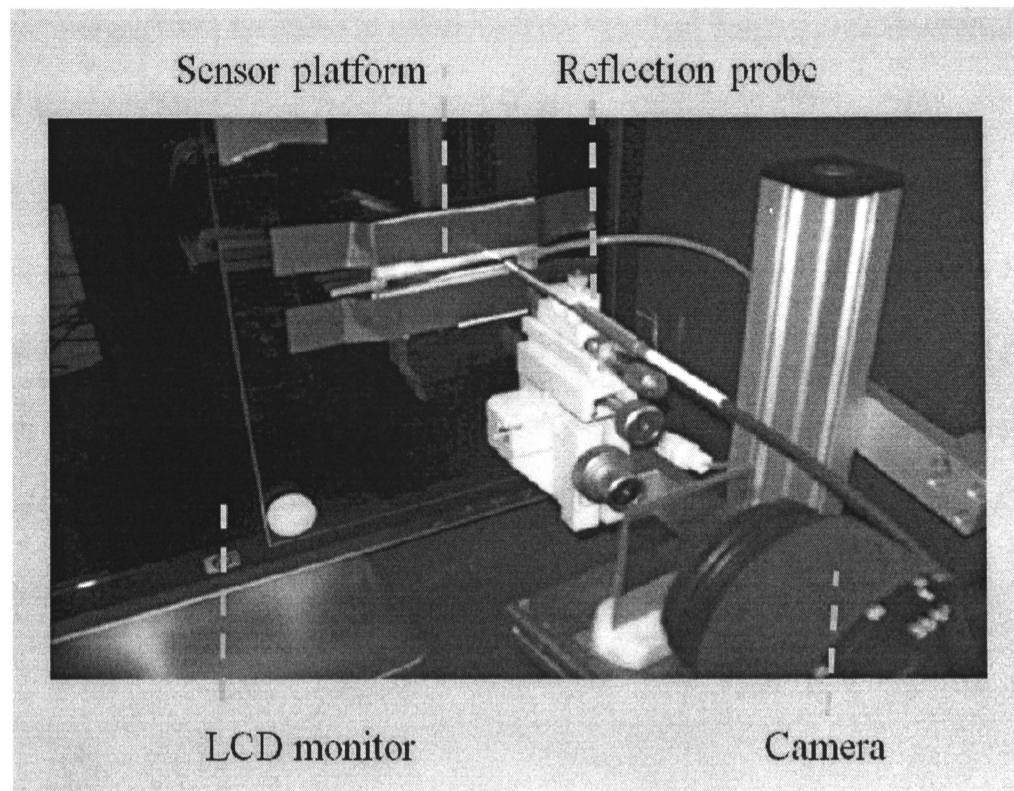


Fig. 2. Photograph of the setup. A camera takes pictures of the sensor patch area in the fluidic sensor platform attached on the surface of the LCD monitor. A reflection probe harvests the emission from the sensor patch area or from the background LCD display.

## **2.4 EXPERIMENTAL PROCEDURE AND ANALYSIS METHOD**

Before conducting the series of experiments, the LCD monitor was turned on for at least five minutes to give a warm up time. The measurements were focused on oxygen percentage between 0% (hypoxic) and 20% (aerated). A gas mixture of a certain ratio of oxygen and nitrogen was purged for 10 minutes. Then, the monitor was turned on to illuminate the blue light for one minute. The picture was taken immediately after stopping the gas flow to eliminate any pressure effect on sensor signals. Twelve continuous images were recorded at a time and the first two images were discarded to eliminate any possible noise caused by the initial warming up of CCD sensor.

A custom MATLAB code was written to crop the region-of-interest (ROI) from the images of the optical oxygen sensor, extract red intensity values and calculate their average values. The ROI of about 60 x 60 pixel size has been cropped from each sensor image and the average red intensity value over the ROI was analyzed. Finally an average red intensity value of ten images taken at a time was used to determine the oxygen concentration.

### 3. RESULTS AND DISCUSSION

#### 3.1 SPECTRAL ANALYSIS OF OXYGEN PATCH SENSITIVITY AND LCD EMISSION

We first characterized the oxygen sensitivity of the commercial oxygen sensor patch and the three elemental color emission from the LCD monitor with a spectrometer and a reflection probe. As shown in Fig. 3, the emission light intensity of the sensor patch changes with respect to the gaseous oxygen contents with an LED excitation light illuminated through the reflection probe.

Figure 4 shows a spectral analysis of three elemental colors displayed from the LCD monitor. The blue color is digitally expressed with an RGB color space value (0, 0, 255) and its wavelength range spans between 430 nm and 480 nm with a peak at 470nm. This indicates that the LCD blue screen can be used as an excitation light source for the ruthenium-complex oxygen sensor patch.

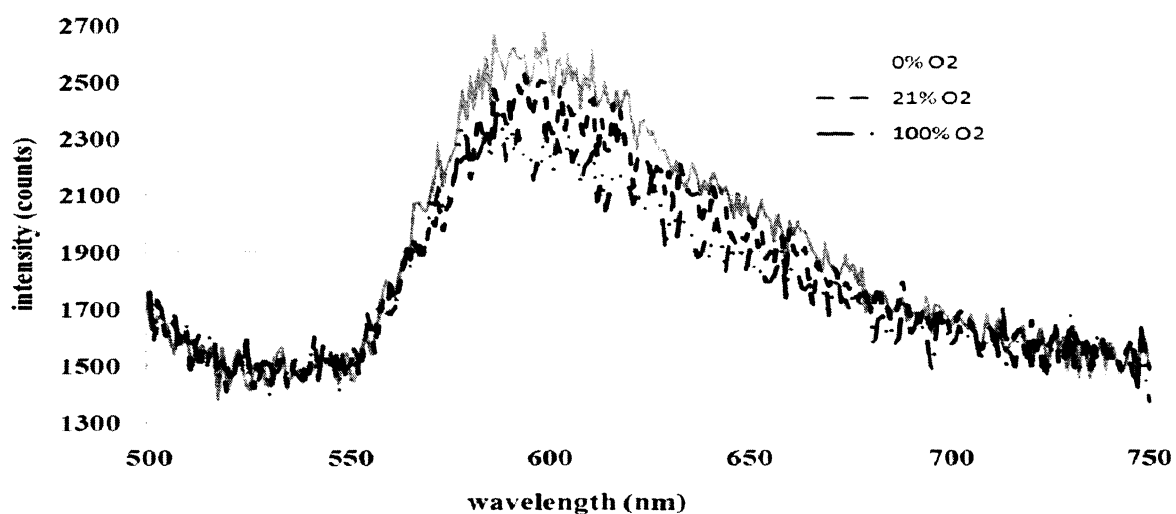


Fig. 3. Spectra of a commercial oxygen sensor patch (RedEye™) taken at various ratios of gaseous oxygen obtained with a spectrometer.

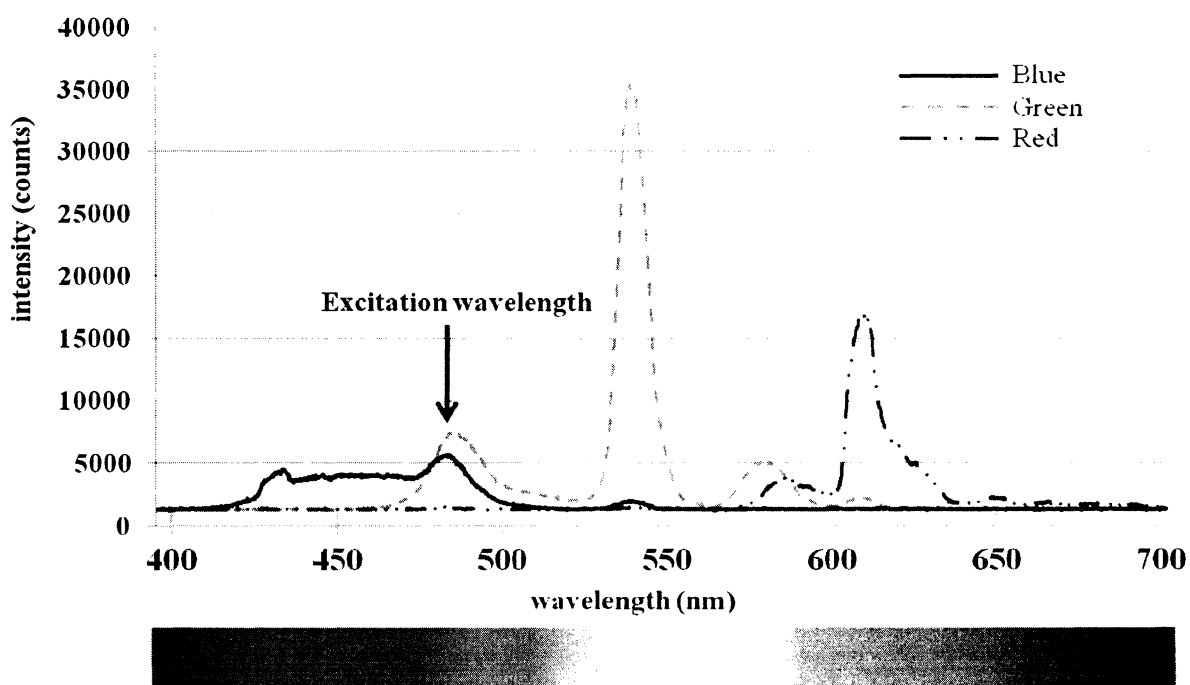


Fig. 4. Spectra of three primary colors (blue, green and red) displayed by an LCD monitor.

### 3.2 SENSOR IMAGE ANALYSIS

Figure 5 shows the cropped ROI images at different gaseous oxygen percentages and red value extracted images along with their histograms. The green tone is dominant in the original images (before red extraction) because of the long pass filter. The histograms clearly indicate the change of red intensities as the peak intensity decreases with respect to oxygen.

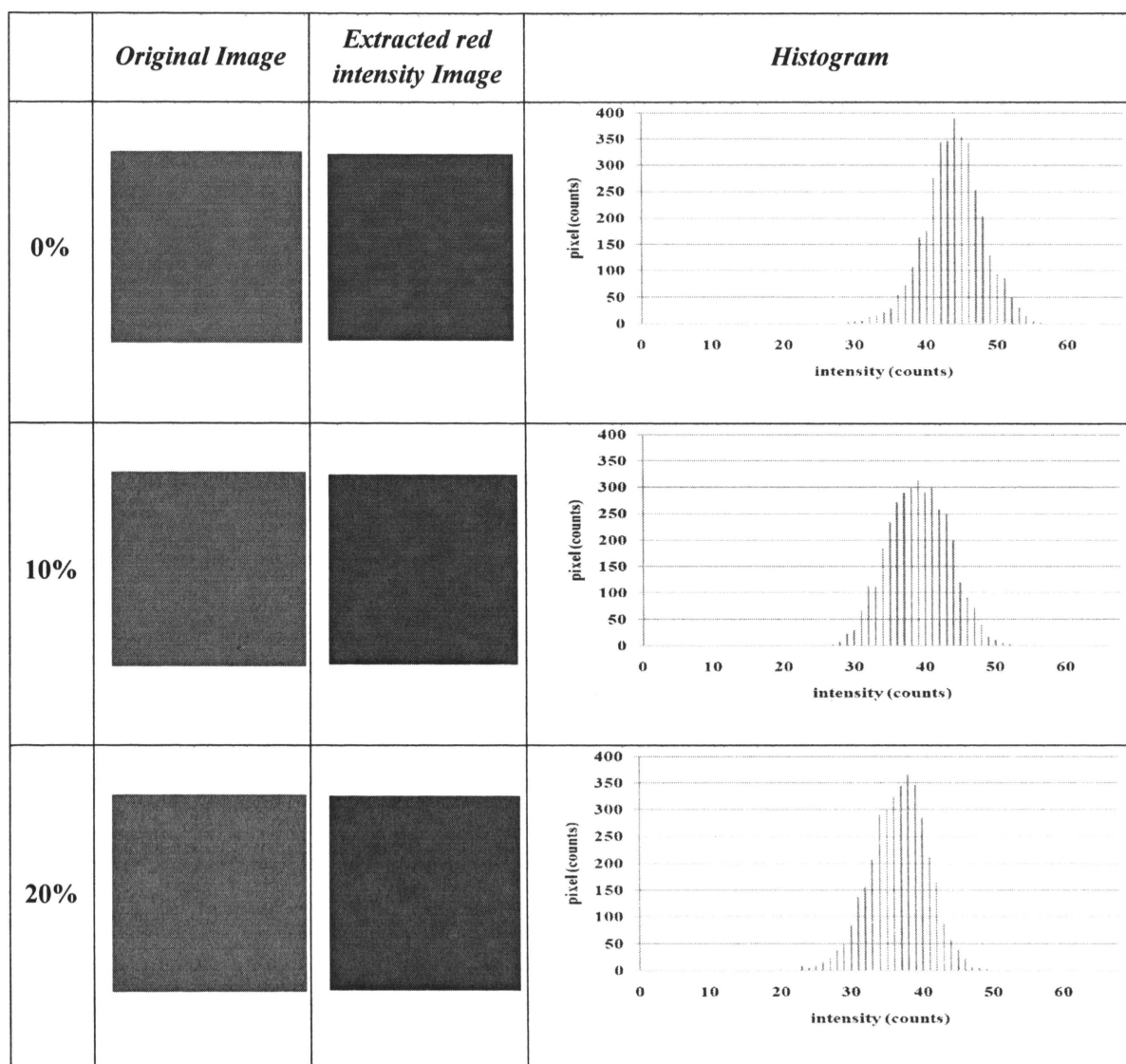


Fig. 5. Cropped ROI images (about 3 mm x 3 mm) at different gaseous oxygen percentages and their histograms.

### 3.3 OXYGEN SENSITIVITY

The oxygen sensitivity was analyzed based on the following Stern-Volmer equation [1]:

$$\frac{I_0}{I} = 1 + K_{sv} [o_2] \quad (1)$$

$$K_{sv} = k_q \tau_0 \quad (2)$$

where  $I_0$  and  $I$  are the fluorescent intensities in the absence and presence of dissolved oxygen molecules, respectively,  $[O_2]$  is the aqueous concentration of dissolved oxygen molecules,  $K_{sv}$  is the Stern-Volmer quenching constant,  $K_q$  is the quencher rate coefficient,  $\tau_0$  is the fluorescence lifetime of the fluorophore without quencher (i.e. oxygen). The advantage of this Stern-Volmer equation is that it can provide normalized values at each oxygen concentration. Red intensities of the acquired digital images of sensor patches may depend on the operation conditions such as camera setting and light source intensity. Normalizing the data using the Stern-Volmer equation, however, can circumvent all these factors. Figure 6 shows the variation in the red color intensity of the ten digital images taken at the same time. Figure 7 shows the Stern-Volmer plot where  $I_0$  is the red intensity of digital images at 0% oxygen condition and  $I$  represents the red intensities at various oxygen percentages. Each data point in Fig. 7 represents an average of the ten values taken at a given condition as in Fig. 6. It is shown that the blue wavelength range (peak 470 nm) emitted from the LCD monitor effectively excites the ruthenium-complex fluorophore in the sensor patch and exhibits a Stern-Volmer relationship.

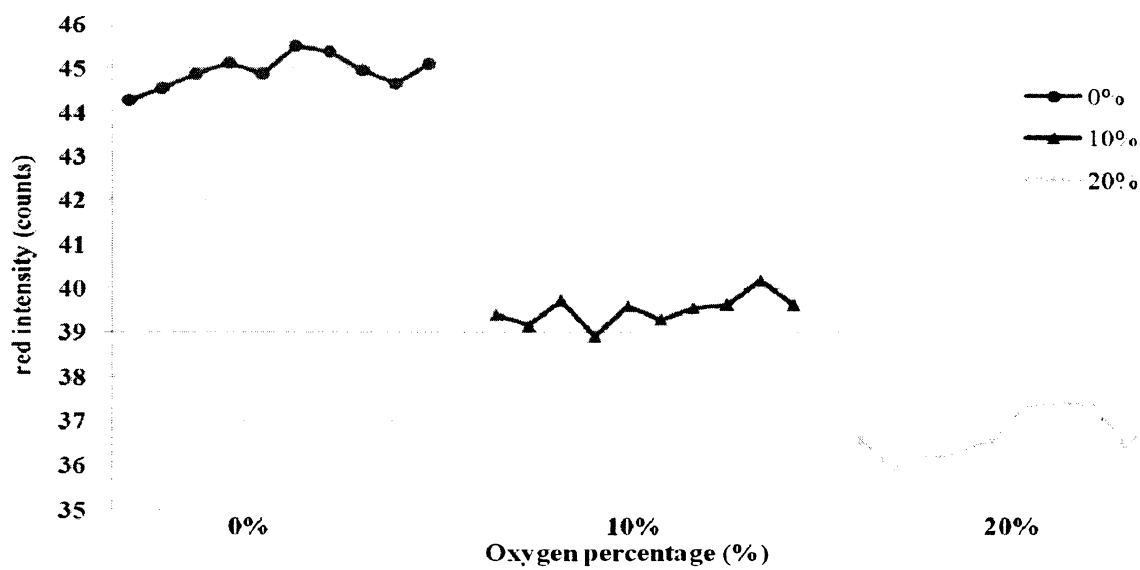


Fig. 6. Variation in the red color intensity of ten images taken at a time at different oxygen percentages.

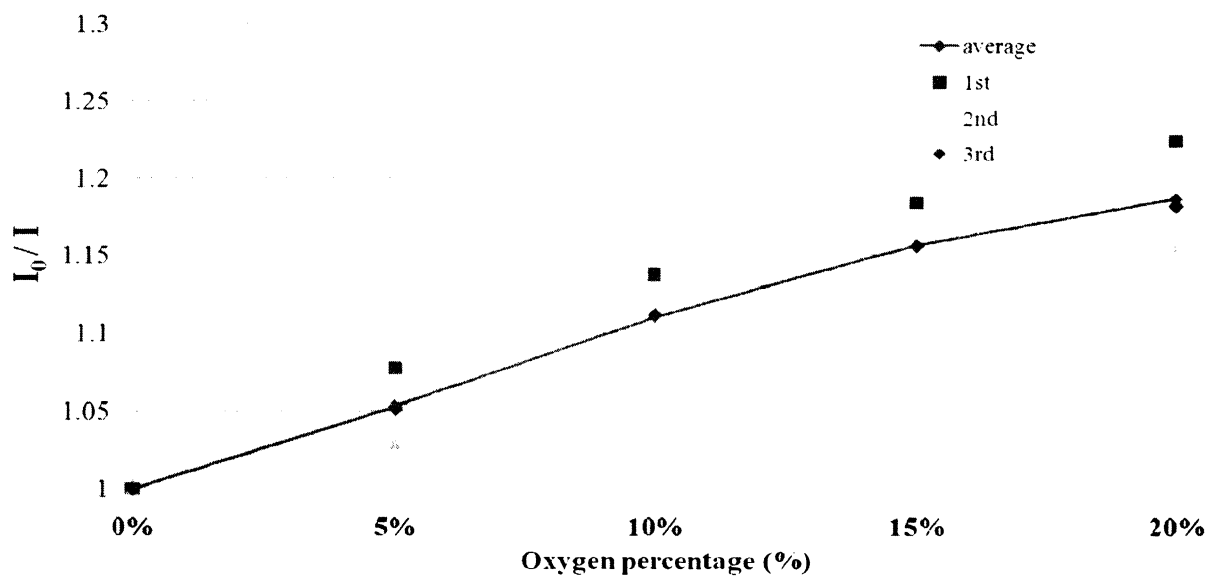


Fig. 7. Stern-Volmer plot of the red intensity of digital images versus gaseous oxygen percentage ( $n=3$ ).

#### 4. CONCLUSION

It was demonstrated that an easily accessible commercial LCD monitor can be used as the light source for quantitative analytical applications. The ruthenium-complex fluorophore immobilized in the commercial oxygen sensor patches is excited by blue wavelength range (about 470 nm peak) emitted from the LCD monitor. A good colorimetric relationship between the red pixel intensity and gaseous oxygen was observed. The capability of uniform illumination over a large area with variable wavelength ranges enables the recording of the spatial distribution of chemicals over a large area and the analysis of multiple target analytes simultaneously. Therefore, the LCD monitors or similar electronic display devices exhibit a great potential as light sources for high-throughput, quantitative, colorimetric chemical analysis.

## REFERENCES

- [1] X-d. Wang, H-x. Chen, Y. Zhao, X. Chen, X-r. Wang, Optical oxygen sensors move towards colorimetric determination, *Trends in Analytical Chemistry*, 29 (4), 319-338, 2010
- [2] J. Manzano, D. Filippini, and I. Lundström, Computer Screen Illumination for the Characterization of Colorimetric Assays, *Sensors and Actuators B - Chemical*, 96 (1-2), 173-179, 2003
- [3] D. Filippini, G. Comina, and I. Lundström, Computer Screen Photo-Assisted Reflectance Fingerprinting, *Sensors and Actuators B – Chemical*, 107 (2), 580-586, 2005
- [4] D. Filippini, J. Bakker, and I. Lundström, Fingerprinting of Fluorescent Substances for Diagnostic Purposes using Computer Screen Illumination, *Sensors and Actuators B - Chemical*, 106 (1), 302-310, 2005
- [5] D. Filippini, and I. Lundström, Preferential Color Substances and Optimized Illuminations for Computer Screen Photo-Assisted Classification, *Analytica Chimica Acta*, 557 (1-2), 393-398, 2006
- [6] S. Macken, I. Lundström, and D. Filippini, Optical Properties of Microstructures for Computer Screen Photoassisted Experiments, *Applied Physics Letters*, 89 (25), 254104, 2006
- [7] E. Gatto, M. A. Malik, C. D. Natale, R. Paolesse, A. D'Amico, I. Lundstrom, D. Filippini, "Polychromatic Fingerprinting of Excitation Emission Matrices." *Chemistry - A European Journal* 14 (20), 6057-6060, 2008
- [8] M. A. Malik, E. Gatto, M. A. Malik, S. Macken, C. DiNatale, R. Paolesse, A. D'Amico, I. Lundstrom, D. Filippini, Imaging Fingerprinting of Excitation Emission Matrices, *Analytica Chimica Acta*, 635 (2), 196-201, 2009
- [9] J. Park, W. Hong, C-S. Kim, Color intensity method for hydrogel optical sensor array, *IEEE Sensors Journal*, 10 (12), 1855-1861, 2010
- [10] X-d. Wang, R. J. Meier, M. Link, O. S. Wolfbeis, Photographing Oxygen Distribution, *Angewandte Chemie - International Edition*, 49 (29), 4907-4909, 2010

- [11] J. Park, C-S. Kim, A simple oxygen sensor imaging method with white light-emitting diode and color charge-coupled device camera, *Sensor Letters*, 9 (1), 118-123, 2011

## II. QUANTITATIVE OXYGEN IMAGING WITH A DISPLAY SCREEN AND A COLOR CAMERA

### ABSTRACT

Familiar optoelectronic devices were utilized to demonstrate a simple determination method of gaseous oxygen both quantitatively and qualitatively. A liquid crystal display (LCD) screen and a color charge-coupled device (CCD) camera were employed as a light source for fluorescence excitation and a photodetector for emission measurement, respectively. Meso-scale test platforms incorporating fluidic channels and oxygen sensor films were prepared. The ruthenium-complex sensor films were excited by blue light displayed from the LCD screen to emit fluorescence responding to gaseous oxygen. The color camera was used successfully to characterize red fluorescence emission from sensor films based on colorimetric intensity measurements. A simple intensity method introduced in this study has an advantage over simplicity of the equipment and is considered a good alternative approach to time-resolved methods for relatively short-term monitoring. This combination of LCD and color camera enables a capability of uniform illumination over a large area with variable wavelength ranges to image spatial distribution of chemicals and to analyze multiple target analytes simultaneously.

### Keywords

optical oxygen sensor, liquid crystal display (LCD), color camera, charge-coupled device (CCD), colorimetry, ruthenium complex

## 1. INTRODUCTION

The oxygen molecule is one of the major metabolites of live organisms and our terrestrial and atmospheric environment. Therefore, there are numerous application fields where oxygen quantification is important. Electrochemical approaches with Clark type or galvanic type oxygen electrodes has been the most common and well-developed techniques for several decades. This electrochemical determination, however, consumes oxygen that may disturb the original sampling environment to be analyzed and is less compatible with two-dimensional analysis. Therefore, optical oxygen sensing is emerging as an alternative approach to be able to overcome these obstacles [1-3]. Optical oxygen sensing uses luminophores such as metal complex dyes that respond to oxygen when illuminated by their specific excitation wavelengths. Emission intensities from these materials are quenched in contact with oxygen molecules. Oxygen contents in samples can then be determined in terms of absolute emission intensity, phase shift of emission or decay lifetime of emission.

Traditional optical instruments for detecting biochemical analytes are mostly spectrometric instruments based on the measurements of luminescence emission, absorption or reflection. Although compact field-use spectroscopy systems are available, the inherent hardware complexity and high costs of such optical systems largely prohibit their common use as simple and economic point-of-care diagnosis devices. Such spectrometry, however, is inherently for one-dimensional point analysis of samples. Therefore, as an alternative and supplementary mean to spectroscopy, there is a great need to develop simple, economical, photometric detection components toward quantitative, multiple-analyte, and two-dimensional mapping instruments. Thanks to the

responsivity and selectivity to a wide range of wavelengths, combined with color imaging software, the color charge coupled device (CCD) and complementary metal oxide semiconductor (CMOS) image sensors exhibit a great potential for photometric chemical quantification. Especially, several reports demonstrated the use of color cameras for colorimetric oxygen determination very recently [4-6]. This was possible because the wavelength range of oxygen-responsive emission almost overlapped with the spectral sensitivity range of red color pixels of digital color imaging devices.

A wide variety of light sources are available for exciting luminophores including broad-band lamps with optical filters and solid-state devices such as light-emitting diodes (LEDs) and laser diodes. For oxygen determination with ruthenium-complex fluorophores, blue LED bulbs (about 470 nm peak) are the most simple and inexpensive option. A white LED was also successfully used without an optical filter for determining gaseous oxygen quantitatively for a specific experimental condition [6]. These types of light sources, however, are limited to one-dimensional illumination over sample surfaces. For mapping the two-dimensional distribution of chemicals, however, a uniform illumination of excitation light over a wide area is critical. Ubiquitous liquid crystal display (LCD) screens can be an excellent candidate for this application with varying color and brightness that can be controlled simply by a computer without any special software. Theoretically, color display screens can implement 16 million different colors by mixing three primary colors of red, green and blue (RGB). New techniques are recently emerging where these devices are applied to chemical quantification purposes. Although it was not focused on two-dimensional mapping, one research group first demonstrated a pioneering concept of computer screen photo-assisted technique (CSPT)

[7-13]. Either cathode ray tube (CRT) or LCD screens were used as illumination light source in these studies for analytical applications based on reflection and emission measurements.

We adopted two familiar optoelectronic devices, a color CCD camera as photodetector and an LCD screen as excitation light source, to determine gaseous oxygen contents and map oxygen distributions. As a proof-of-concept model system, we prepared meso-scale sensor platforms with fluidic channels over oxygen sensor coated glass plates. These sensor platforms were attached on the LCD surface and the oxygen distributions were analyzed both qualitatively and quantitatively over a wide area. Ruthenium-complex fluorophores immobilized in sensor coatings were excited by the blue wavelength range (about 470 nm peak) from the LCD screen. Digital images of the two-dimensional sensor surface were acquired and their red pixel intensities were analyzed for oxygen determination.

## 2. EXPERIMENTS

### 2.1 MATERIALS AND EQUIPMENT

**2.1.1 Oxygen Sensor Coating.** Ru(II)-complex fluorophores, dichlorotris (1,10-phenanthroline) ruthenium(II) hydrate (98%, Sigma-Aldrich), one of the metal-complex organic dyes most frequently used for oxygen detection, was used as the oxygen-selective agent. This material was chosen because its peak excitation wavelength about 470 nm can be readily provided by the LCD screen. An oxygen sensor cocktail was prepared by mixing ruthenium-complex powder, toluene, silica particles (Cab-O-Sil fumed silica EH-5, Mozel) and two-part silicone (Sylgard 184, Dow Corning). The silicone was used for immobilizing the fluorophore, ruthenium. Since ruthenium-complex is not uniformly soluble in silicone, it is loaded onto silica particles before being evenly mixed with the silicone. Toluene was used as the solvent to physically adsorb the ruthenium particles onto silica.

First, ruthenium-complex (3.75 mg) was dissolved in 10 ml toluene in a brown glass bottle and stirred for 30 minutes. After that, fumed silica particles (0.6 g) were added and stirred overnight. A small amount of silicone was mixed with its curing agent (10:1 ratio) and placed in a vacuum chamber to remove air bubbles. This two-part silicone (6.6 ml) was added into the mixture and stirred for 30 minutes. This final sensor cocktail was then ready for coating on glass plates (70 mm x 50 mm and 150 mm x 100 mm). It was spin coated at 300 rpm for 10 seconds for uniform thickness. Finally, the sensor-coated plates were baked at 65 °C for 30 minutes on a hot plate for curing.

**2.1.2 Sensor Platform.** Two different types of meso-scale fluidic sensor platforms were prepared. The first type was a meso-scale rectangular fluidic sensor platform with two gas channels on its left and right sides. As shown in Fig. 1 (a), it consisted of two glass plates (150 mm x 100 mm x 1 mm), several pieces of rubber spacers (2 mm thick), two porous sponge sheets (Z80CH, 3 mm thick, McMaster-Carr: this is a distributor, not a manufacturer) and polyethylene tubing (inner diameter 1/8"). Gas fluidic channels were formed between the two glass plates utilizing the rubber spacer as the channel wall. Pieces of polyethylene tubings were used as gas inlets and outlets. The optical sensor cocktail was coated on the entire surface of the bottom glass plate. All components were glued with a two-part epoxy (or instant glue). This arrangement created a rectangular sensor area (i.e. middle compartment: 60 mm x 90 mm) and two gas channels (i.e. left- and right-side compartments: 100 mm x 5 mm) separated by a porous sponge areas (5 mm wide). It was designed to create a two-dimensional oxygen gradient over the rectangular area by the two channels through which two different gases with different oxygen ratios flowed. The sponge served as a gas permeable region from the outer channels into the rectangular area. To minimize any positive pressure buildup and expedite the gas exchange, discontinuities were made within the rubber spacer.

The second type is a Y-junction sensor platform. It was designed to create a laminar flow inside a merged main channel with two gas influxes of different oxygen ratios. The primary structure mimics the rectangular platform as shown in Fig. 1 (b). It consisted of two standard size glass slides (75 mm x 50 mm x 1 mm) and other components same as explained previously. It shows a main channel (40 mm x 10 mm) with two input channels (5 mm wide) with a 30 degree angle between them.

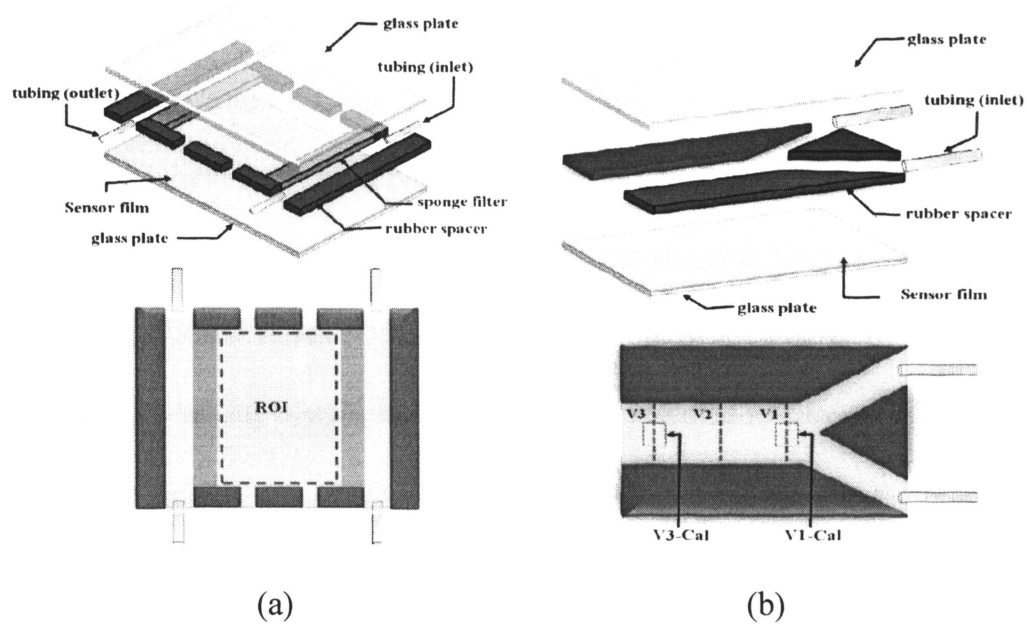


Fig. 1. Two types of meso-scale, gas fluidic sensor platforms (not in real scale). (a) Structure and layout of a rectangular sensor and channels to induce a two-dimensional oxygen gradient over a region of interest (ROI) (area: 60 mm x 90 mm). (b) Structure and layout of a Y-junction sensor to induce a laminar flow in the merged main channel (width: 40 mm) and two calibration areas (3 mm x 3 mm).

**2.1.3 Liquid Crystal Display.** A thin film transistor liquid crystal display (TFT LCD) screen (HP 2159m, 21.5" color LCD monitor, Hewlett-Packard) was used as the excitation light source. TFT LCD has a liquid crystal layer sandwiched in between the TFT glass plate and the color filter plates. The light intensity is controlled by liquid crystal polarization by voltage between the two glass plates. Cold cathode fluorescent lamps (CCFLs) or LEDs are commonly used for backlight and a color filter layer which generates colors. LCD screens use three color filters (red, green, blue) and mixes three major wavelengths to display true color (i.e.  $256 \times 256 \times 256 = 16,777,216$  different colors with 24-bit RGB color space). Size of dot pitch (e.g. 0.248 mm for this product) is the primary factor for our purpose because smaller pitch provides more uniform intensity

over the screen area. Through this study, we displayed blue color of which the wavelength range spans between 430 nm and 480 nm with a peak at 470 nm.

**2.1.4 Color Camera.** Color CCDs have built-in, on-chip filter arrays of three elemental colors. Each color filter passes its specific wavelength light to an individual photosensor element and the number of photons is translated in terms of voltage. We used a digital single-lens reflex (DSLR) camera ( $\alpha$ 350 DSLR camera, 14.2 Megapixel, Sony). All camera setting conditions were manually selected as shown in Table 1 to prevent any automatic image correction. The International Standards Organization (ISO) number represents the duration of active mode of the photosensor. The sensitivity of the photosensor increases with a higher ISO number. Shutter speed determines exposure time of the photosensor to light. The white balance function compensates for the effect of background lighting on digital images and is not a physically controlled mechanism. The f-number is the focal length divided by the effective aperture diameter. A larger f-number indicates less light reaching the photosensor. The setting values were chosen after a series of tests and optimized for our experimental conditions.

It is known that the red pixel is also sensitive over the blue and green wavelength ranges although the sensitivity is very limited. Therefore, a long pass filter (OG550, cut-off wavelength 550 nm, 2" x 2", Thorlabs) was placed in front of camera to remove the strong blue excitation wavelength. This filter is also expected to minimize the CCD noise caused by the light below the cut-off wavelength.

Table 1. Optimized CCD camera setting conditions used for this study.

Parameters	ISO	Shutter speed	White balance	F-number	Focus
Setting values	400	0.8 seconds	Sunlight	5.6	focused

## 2.2 CHARACTERIZATION

**2.2.1 Measurement Procedure.** The measurement setup is shown in Fig. 2. A large glass plate (1.5 mm thick) was attached to the LCD screen with elastic spacers (5 mm thick) and the fluidic sensor platform was placed on the glass plate surface. The use of this glass plate between LCD screen and sensor platform was to minimize the dependence of sensor emission on temperature change caused by thermal radiation from the screen. The long pass filter was placed in close proximity to the camera lens to remove the strong blue excitation light. The whole setup was placed in a dark chamber to minimize any effect of stray light.

We performed two kinds of experiments using the rectangular sensor and the Y-junction sensor platforms. Each experiment consisted of an initial calibration procedure and the main measurement procedures. The LCD screen was initially warmed up for about five minutes to emit light with stable intensity before measurements. A gas mixture of a certain oxygen percentage (i.e. different ratios of oxygen and nitrogen) was purged inside the channel through inlet tubings for a certain period depending on the experiments.

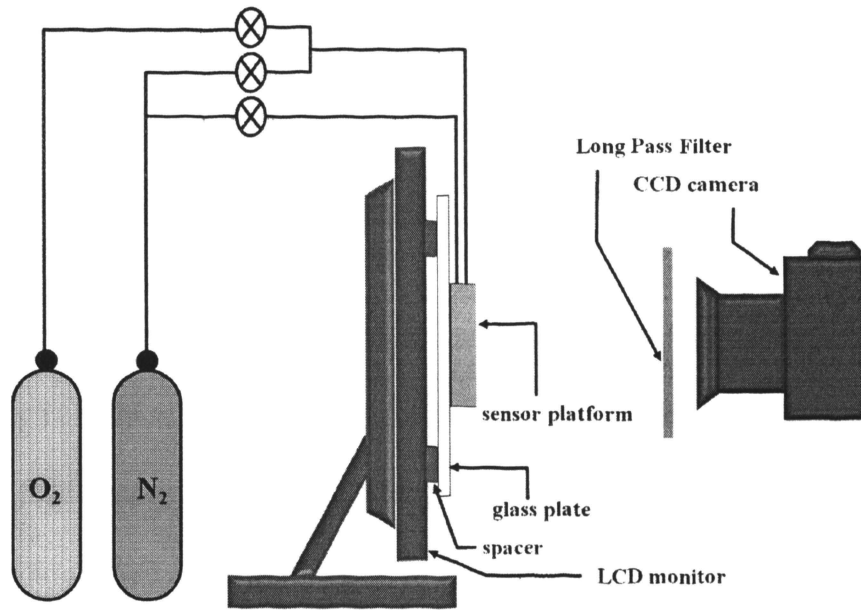


Fig. 2. A color camera takes pictures of the fluidic sensor platform installed in close proximity to an LCD screen that provides an excitation light with uniform intensity over the sensor coating.

Then, the screen displayed the blue light for one minute, immediately followed by taking pictures before the screen was turned off. Ten pictures were taken continuously at a time for averaging, which took less than twelve seconds.

**2.2.2 Image Analysis Procedure.** Oxygen concentration can be determined from optical oxygen sensors by measuring intensity, lifetime or phase shift based on the Stern-Volmer relationship as follows [14]:

$$I_0/I (= \tau_0/\tau = \Phi_0/\Phi) = 1 + K_{SV} [O_2] \quad (1)$$

where  $I_0$  and  $I$  ( $\tau$ ,  $\Phi$ ) represent the steady-state fluorescence emission intensities without and with the quencher (here oxygen). Alternately,  $\tau$  and  $\Phi$  mean the lifetime (decay time) of fluorescence when a constant excitation light is switched off and the phase angle shift of fluorescence (time delay) from a sinusoidal excitation light caused by its decay lifetime, respectively.  $K_{sv}$  is the Stern-Volmer quenching constant and  $[O_2]$  is the oxygen concentration, respectively. Therefore, the ratio of fluorescence intensities

without and with oxygen ( $I_0/I$ ) becomes linearly proportional to the oxygen concentration.

Custom MATLAB codes were written for pre-processing the images and reconstructing oxygen distribution images. MATLAB codes are made for each sensor platform and process. The scheme of overall processing is shown in appendix. C. Digital images usually contained noise pixel values that were caused from various sources including the CCD image sensor, the LCD screen and other random, uncontrollable sources. This noise was significantly reduced with a pre-processing step based on a simple averaging technique. Ten continuous photographs were taken at a time for each measurement and all images were averaged to generate a new “average image”. In other words, each pixel value in this average image is the average of ten pixel values of the same coordinate in ten images. Therefore it is very critical that the field-of-view of the camera does not change during the continuous photographing. To reconstruct this information to qualitative oxygen distribution images, we adopted the Stern-Volmer relationship. To do this, an image with the entire sensor area fully saturated with nitrogen (i.e. no oxygen; equivalent of  $I_0$  in Eq. 1) was taken first. This image was then divided by another image with a different gas environment (i.e. equivalent of  $I$  in Eq. 1) to reconstruct a “Stern-Volmer image” (i.e. equivalent of  $I_0/I$  in Eq. 1) that shows the oxygen distribution qualitatively. For quantitative analysis with the Y-junction sensor, a calibration procedure with five different gas compositions was conducted with the oxygen percentage ranging between 0% and 20%. The calibration gases were sequentially perged through the inlet for ten minutes per each gas composition. A small region (100 x 100 pixels) in the middle of the main channel was cropped and the average

red intensity of all pixels within this region was used as the calibration value of each gas composition.

### 3. RESULTS AND DISCUSSION

#### 3.1 OXYGEN SENSOR PATCH ANALYSIS

We first characterized the three elemental color emissions from the LCD screen with an optical fiber spectrometer placed in front of the screen. Figure 3 shows spectral analysis of three elemental colors emitted from the LCD screen. The blue color is digitally expressed as (0, 0, 255) in terms of RGB color space and its wavelength range spans between 430 nm and 480 nm with a peak around 470 nm. Therefore, it is expected that the blue color emission from the LCD screen can be used to excite the ruthenium-complex fluorophore for emission responding to oxygen.

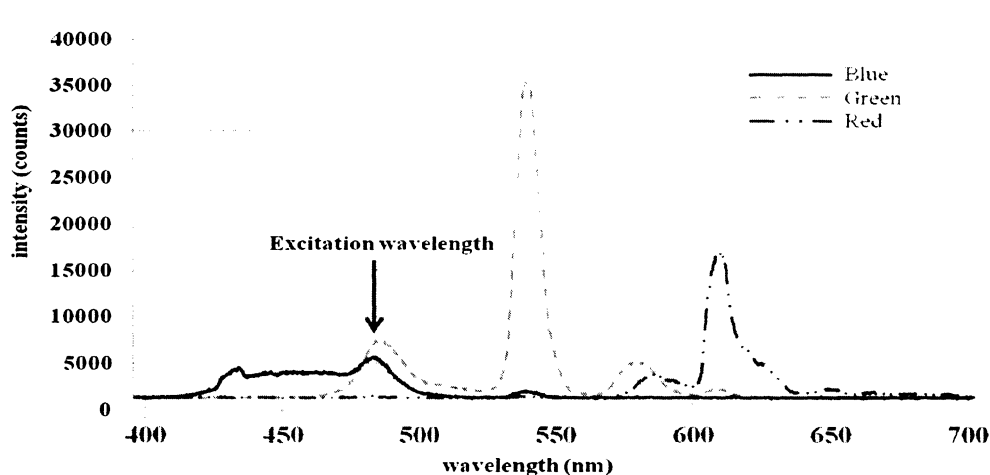


Fig. 3. Spectra of three primary colors (blue, green and red) displayed by an LCD screen. The ruthenium-complex fluorophore is excited for emission around 470 nm.

As a preliminary proof-of-concept test, we characterized the oxygen sensitivity of a commercially available sensor patch with this setup. An oxygen sensor patch (RedEye™, RE-FOX-8, 8 mm diameter, OceanOptics) employs the ruthenium-complex oxygen-responsive fluorophore. This patch was attached within the channel of the fluidic platform instead of the laboratory-prepared sensor coating. All the measurements were focused on the biological oxygen range of 0% (hypoxic) to 20% (aerated) oxygen percentage. As explained in the previous section, ten images at a given condition were pre-processed to generate an average image for noise reduction. A region of interest (ROI) of 60 x 60 pixel size within the sensor patch area was cropped to average the red intensity values of all pixels inside the ROI. Figure 4 is a plot of the ratio ( $I_0/I$ ), with  $I_0$  and  $I$  being the average red intensities inside the ROI in the absence and presence of oxygen, respectively. Ideally, this plot should exhibit a linear relationship between  $I_0/I$  and oxygen as described in Eq. 1. There are many practical factors involved in this commonly downward curve and several plausible models have been reported to explain this phenomenon [15-17]. This implies that the combination of an LCD screen and a color camera can be used for colorimetric oxygen quantification.

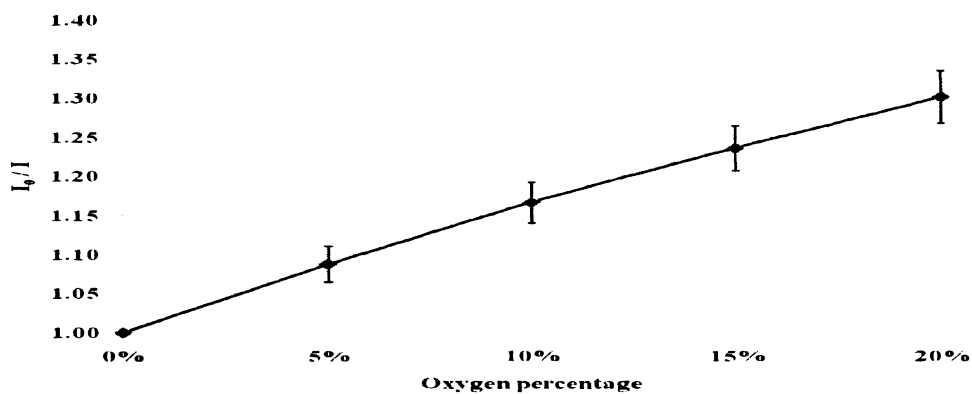


Fig. 4. Stern-Volmer plot of the red intensity of a commercial oxygen sensor patch (RedEye™) versus gaseous oxygen percentage (n=4).

### 3.2 RECTANGULAR SENSOR PLATFORM

The experiment with the rectangular sensor platform was focused on imaging oxygen distribution qualitatively over a meso-scale area. Initially, the entire sensor platform was completely saturated with nitrogen environment (i.e. 0% oxygen) to obtain a reference image of the rectangular sensor area (i.e. equivalent of  $I_0$  in Eq. 1). This was done by closing the outlet tubings to fill out the rectangular area completely with the nitrogen gas for 30 minutes. Figure 5 (a) is the pre-processed average image of the ten ROI images taken at a time with nitrogen saturated environment. The brighter area in the middle was caused by non-uniform sensor coating thickness that gives a higher fluorescence intensity than the rest of sensor area. Then, at  $t = 0$  second, both outlets were opened to allow a slow flow of nitrogen and 20% oxygen gases through the left- and right-side channels, respectively. Figure 5 (b) shows that the fluorescence emission from the right side became quenched by oxygen permeated through the porous sponge layer at  $t = 300$  seconds after the gas flow.

Figure 5 (e) is a reconstructed Stern-Volmer image created by the pixel-to-pixel division of digital data of Fig. 5 (a) at  $t = 0$  with those of Fig. 5 (b) at  $t = 300$  (i.e. equivalent of  $I_0/I$  in Eq. 1). The variation of absolute intensities caused by the uneven coating thickness can thus be eliminated by this ratio-based presentation according to the Stern-Volmer relationship in Eq. 1. Figure 5 (c) and (d) represents the temporal variation of oxygen permeation process that spreads out from the right side to the left side of rectangular area. Thus the visualization of oxygen distribution was possible with a combination of these familiar optoelectronic instruments.

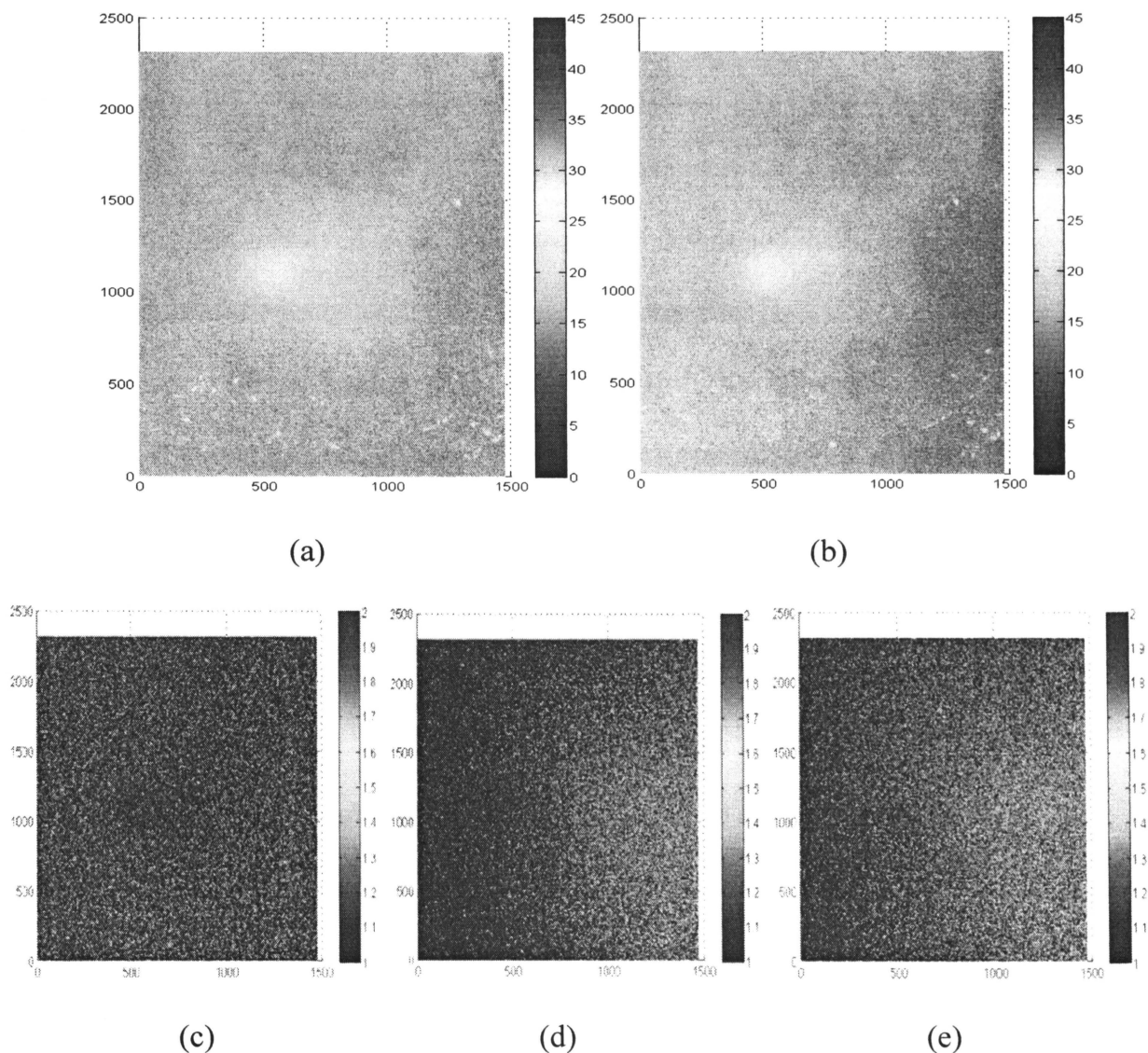


Fig. 5. Visualization of oxygen distribution over the rectangular sensor area as defined in Fig. 1 (a) (60 mm x 90 mm). (a) Red intensity image in a nitrogen saturated environment at  $t = 0$  second (equivalent of  $I_0$ ). (b) Red intensity image with a nitrogen flow (left channel) and 20% oxygen flow (right channel) at  $t = 300$  seconds (equivalent of  $I$ ). (c) Reconstructed Stern-Volmer image at  $t = 30$  seconds (equivalent of  $I_0/I$ ), (d)  $t = 120$  seconds, (e)  $t = 300$  seconds.

It is known that the absolute intensity measurement suffers from the drift issue over time due to photobleaching or leaching of luminophores and fluctuation of excitation light source intensity. To circumvent this instability issue of intensity measurements, time-resolved techniques have been developed including the luminescence lifetime imaging and the phase shift imaging [1-3,18]. As shown in Eq. (1), theoretically the ratios of lifetime ( $\tau_0/\tau$ ) and phase shift ( $\Phi_0/\Phi$ ) are also linearly proportional to oxygen concentration. The lifetime or phase shift imaging method records the two-dimensional distributions of the decay time or phase shift of luminescence responding to their respective excitation source. Then, an image of the lifetime or the phase shift distribution is reconstructed for visualization over an area to be analyzed. Therefore, special excitation light sources operated by pulse and sinusoidal waves and synchronized high-speed cameras are required for these time-resolved methods. A simple intensity method introduced in this study, however, has an advantage over simplicity of the equipment, thus it is considered a good alternative approach for relatively short-term monitoring.

### 3.3 Y-JUNCTION SENSOR PLATFORM

As demonstrated in the previous rectangular sensor, an oxygen distribution image of the Y-junction sensor was also created. Figure 6 (a) is the red intensity image of the completely nitrogen-saturated channel by the nitrogen influx from both inlets (equivalent of  $I_0$ ). As previously explained, the uneven sensor coating exhibited a variation of intensity over the channel area. When the nitrogen gas influx in the upper branch channel

had been switched to 20% oxygen gas influx for about twenty minutes, keeping the same nitrogen flow through the lower branch, a clear difference in red intensity was observed as in Fig. 6 (b). A Stern-Volmer image was created by the same way as the previous rectangular sensor. In the main channel shown in Fig. 6 (c), the boundary between nitrogen and 20% oxygen gases became more blurred as the flow proceeded.

For quantitative analysis, calibration data is required. As defined in Fig. 1 (b), two calibration areas (3 mm x 3 mm) were cropped and its average red intensity within each area was analyzed. The protocol of this step is same as described in the previous section of commercial sensor patch analysis. Figure 6 (d) compares two calibration curves obtained from the two different areas. It was noticed that this ratiometric Stern-Volmer sensitivities ( $I_0/I$ ) with respect to oxygen were kept very similar with little dependency on the variation of absolute intensities ( $I_0$  and  $I$ ) caused by different sensor coating thicknesses used in this study.

Various parameters required for quantitative analysis of selected areas are plotted in Fig. 7. First, Fig. 7 (a) shows vertical profiles of absolute red intensities across the main channel at three different locations of V1, V2 and V3 defined in Fig. 1(b). In this case all channels are saturated with nitrogen gas being purged from both branches, which exhibits flat intensity profiles across the channel.

The value was higher at V1 location, which was evidenced by Fig. 6 (a) as the sensor coating was thicker in that region. Figure 7 (b) shows the changes in profiles with 20% oxygen flow through the lower branch.

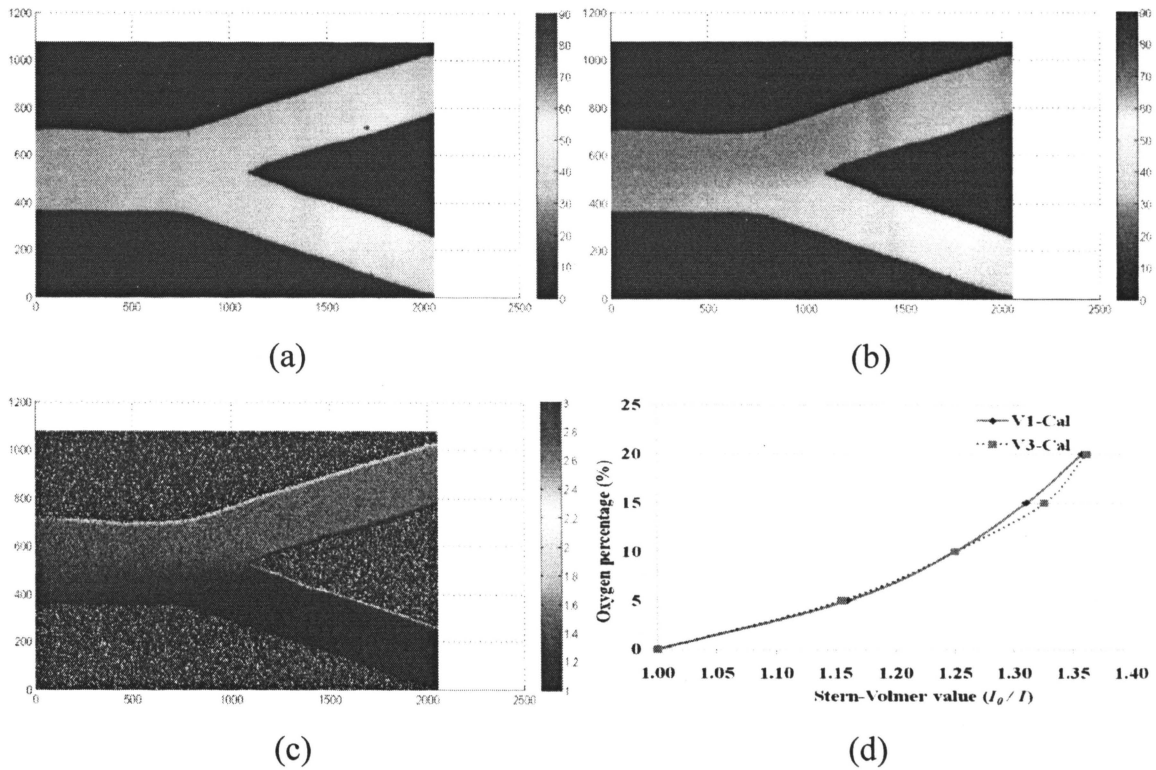


Fig. 6. Images of Y-junction sensor and calibration curves for quantitative analysis. (a) Reference red intensity image with nitrogen flow in both branches (equivalent of  $I_0$ ). (b) Red intensity image with 20% oxygen flow in lower branch and nitrogen flow in upper branch (equivalent of  $I$ ). (c) Stern-Volmer image of oxygen distribution (equivalent of  $I_0 / I$ ). (d) Calibration curves calculated from a calibration area (V1-Cal) in Fig. 1 (b).

Each Stern-Volmer plot in Fig. 7 (c), obtained by dividing each (a) plot by corresponding (b) plot, were finally converted to oxygen percentage profiles in Fig. 7 (d) by fitting them with the calibration curve of Fig. 6 (d). It is clearly observed that there is a difference in the slope across the channel at three locations and that the maximum and minimum values at both ends change. It means that the two gases with different compositions gradually spread into other sides to become more homogeneous at the outlet.

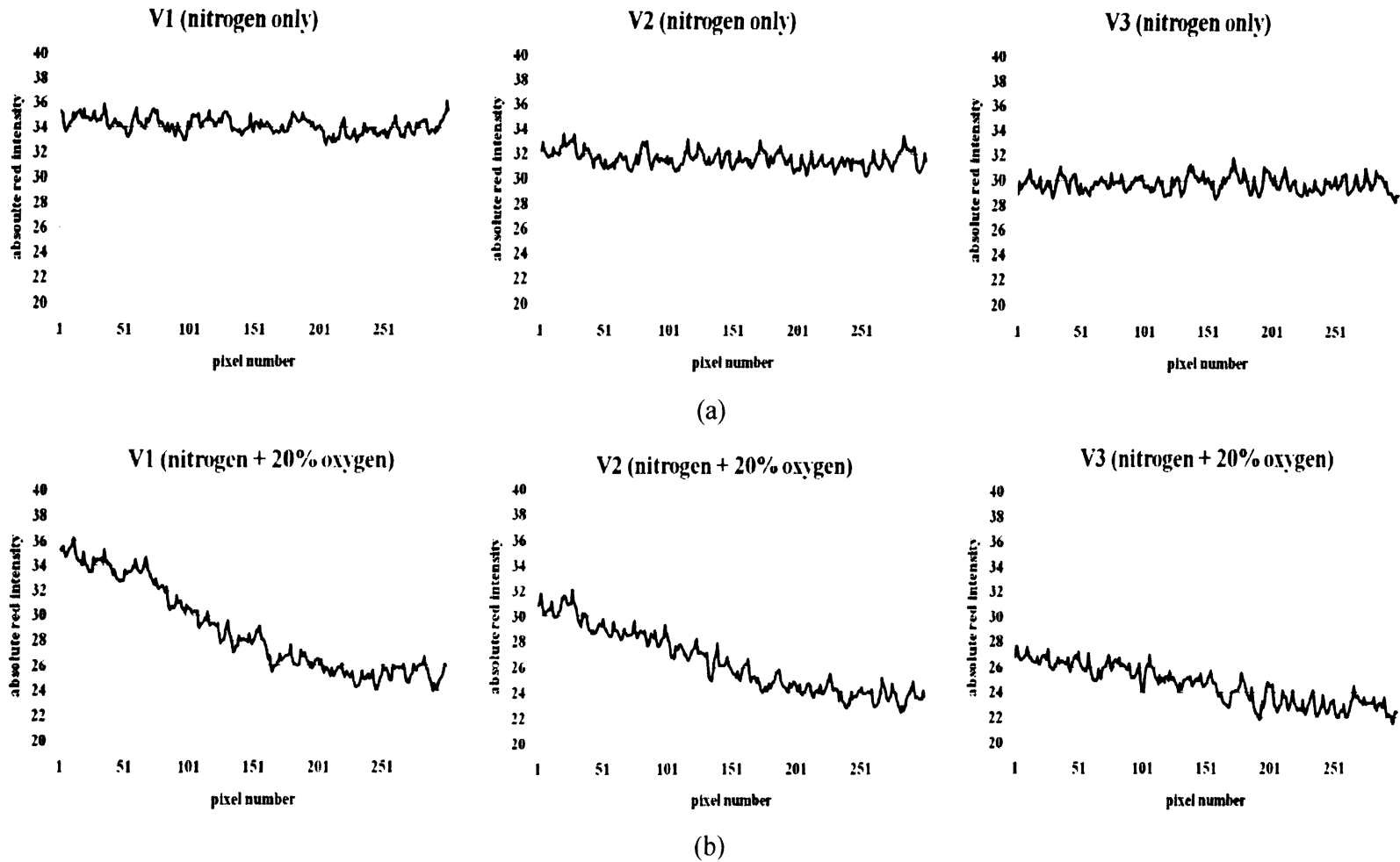


Fig. 7. Vertical profiles of various parameters across the Y-junction main channel at three locations of V1, V2 and V3 defined in Fig. 1(b). (a) Red intensities with nitrogen influx from both branches (equivalent of  $I_0$ ). (b) Red intensities with 20% oxygen influx at one branch (equivalent of  $I$ ). (c) Stern-Volmer values: plot (a) divided by plot (b) (equivalent of  $I_0 / I$ ). (d) Estimated oxygen profile based by fitting plot (c) to the calibration curve.

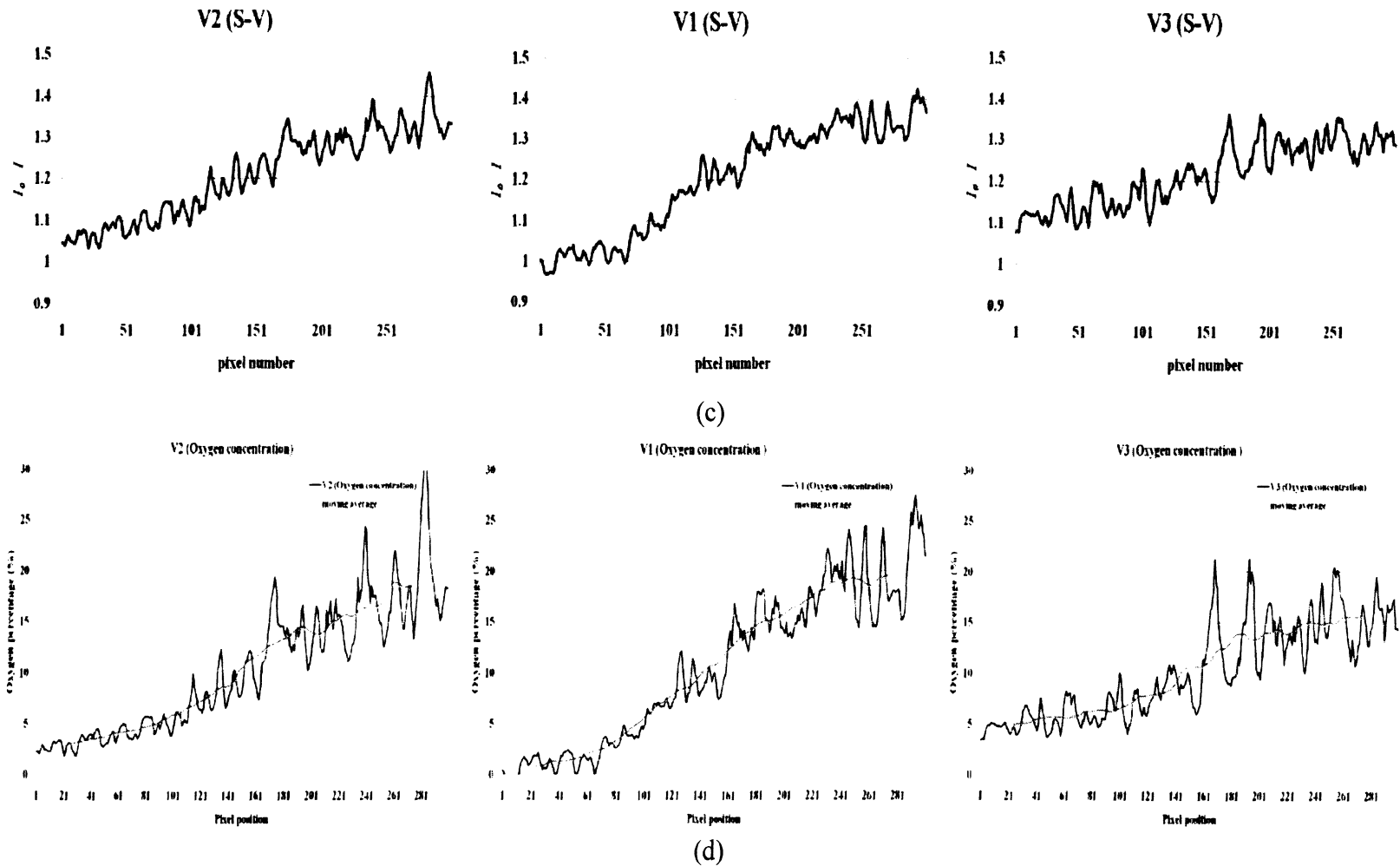


Fig. 7. Vertical profiles of various parameters across the Y-junction main channel at three locations of V1, V2 and V3 defined in Fig. 1(b). (a) Red intensities with nitrogen influx from both branches (equivalent of  $I_0$ ). (b) Red intensities with 20% oxygen influx at one branch (equivalent of  $I$ ). (c) Stern-Volmer values: plot (a) divided by plot (b) (equivalent of  $I_0 / I$ ). (d) Estimated oxygen profile based by fitting plot (c) to the calibration curve. (Continue)

#### 4. CONCLUSION

It was demonstrated that a combination of two easily accessible optoelectronic devices, a commercial LCD screen and a color CCD camera, can be used for gaseous oxygen determination. The laboratory-prepared ruthenium-complex sensor coating was successfully excited by blue light emitted from the LCD screen to emit oxygen-responsive fluorescence emission. The color camera provided significant advantages to store colorimetric digital data with two-dimensional information and analyze its color change and gradient over a captured image area. Both qualitative and quantitative analyses were possible with relatively simple colorimetric image analysis. Therefore, the LCD monitors and the color cameras exhibit a great potential as the inexpensive colorimetric chemical instruments with unique features of large-area and high-throughput analysis.

**REFERENCES**

- [1] Gerhard Holst, Bjorn Grunwald, "Luminescence lifetime imaging with transparent oxygen optodes," *Sensors and Actuators B*, 74, 78-90, 2001
- [2] Paul Hartman, Werner Ziegler, Gerhard Holst, Dietrich W. Lubbers, "Oxygen flux fluorescence lifetime imaging," *Sensors and Actuators B*, 38-39, 110-115, 1997
- [3] Gregor Liebsch, Ingo Klimant, Bernhard Frank, Gerhard Holst, Otto S. Wolfbeis, "Luminescence lifetime imaging of oxygen, pH, and carbon dioxide distribution using optical sensors," *Applied spectroscopy*, 54(4), 549-559, 2000
- [4] J. Park, W. Hong, C-S. Kim, "Color intensity method for hydrogel optical sensor array," *IEEE Sensors Journal*, 10 (12), 1855-1861, 2010
- [5] X-d. Wang, R. J. Meier, M. Link, O. S. Wolfbeis, "Photographing Oxygen Distribution," *Angewandte Chemie - International Edition*, 49 (29), 4907-4909, 2010
- [6] J. Park, C-S. Kim, "A simple oxygen sensor imaging method with white light-emitting diode and color charge-coupled device camera," *Sensor Letters*, 9 (1), 118-123, 2011
- [7] J. Manzano, D. Filippini, and I. Lundström, "Computer Screen Illumination for the Characterization of Colorimetric Assays," *Sensors and Actuators B - Chemical*, 96 (1-2), 173-179, 2003
- [8] D. Filippini, G. Comina, and I. Lundström, "Computer Screen Photo-Assisted Reflectance Fingerprinting," *Sensors and Actuators B – Chemical*, 107 (2), 580-586, 2005
- [9] D. Filippini, J. Bakker, and I. Lundström, "Fingerprinting of Fluorescent Substances for Diagnostic Purposes using Computer Screen Illumination," *Sensors and Actuators B - Chemical*, 106 (1), 302-310, 2005
- [10] D. Filippini, and I. Lundström, "Preferential Color Substances and Optimized Illuminations for Computer Screen Photo-Assisted Classification," *Analytica Chimica Acta*, 557 (1-2), 393-398, 2006

- [11] S. Macken, I. Lundström, and D. Filippini, "Optical Properties of Microstructures for Computer Screen Photoassisted Experiments," *Applied Physics Letters*, 89 (25), 254104, 2006
- [12] E. Gatto, M. A. Malik, C. D. Natale, R. Paolesse, A. D'Amico, I. Lundstrom, D. Filippini, "Polychromatic Fingerprinting of Excitation Emission Matrices," *Chemistry - A European Journal* 14 (20), 6057-6060, 2008
- [13] M. A. Malik, E. Gatto, M. A. Malik, S. Macken, C. DiNatale, R. Paolesse, A. D'Amico, I. Lundström, D. Filippini, "Imaging Fingerprinting of Excitation Emission Matrices," *Analytica Chimica Acta*, 635 (2), 196-201, 2009
- [14] E.R. Carraway, J.N. Demas, B.A. DeGraff, J.R. Bacon, "Photophysics and photochemistry of oxygen sensors based on luminescent transition metal complexes," *Anal. Chem.* 63, 337-342, 1991
- [15] Eun Jeong Cho, Frank V. Bright, "Integrated chemical sensor array platform based on a light emitting diode, xerogel-derived sensor elements, and high-speed pin printing," *Analytica Chimica Acta*, 470, 101-110, 2002
- [16] Volker Nock, Richard J. Blaikie, Tim David, "Patterning, integration and characterization of polymer optical oxygen sensors for microfluidic devices," *The Royal Society of Chemistry*, 8, 1300-1307, 2008
- [17] David D. Bernhard, Shalini Mall, Paul Pantano, "Fabrication and characterization of microwell array chemical sensors," *Analytical Chemistry*, 73, 2484-2490, 2001
- [18] Chen-Shane Chu, Yu-Lung Lo, "2D full-filled measurement of oxygen concentration based on the phase fluorometry technique that uses the four-frame integrating-bucket method," *Sensors and Actuators B*, 147, 310-315, 2010

## SECTION

### 2. CONCLUSION

A combination of two easily accessible optoelectronic devices, a commercial LCD screen and a color CCD camera, was successfully used for gaseous oxygen determination. Meso-scale device platforms are prepared with glass plates incorporating fluidic channels and commercial oxygen sensor patches. The ruthenium-complex fluorophore immobilized in the commercial oxygen sensor patches were excited by the blue color (about 470 nm peak) displayed from the LCD monitor. The color camera provided significant advantages to store colorimetric digital data of fluorescence emission responding to oxygen (about 600 nm peak) with two-dimensional information.

Both qualitative and quantitative analyses were possible with relatively simple colorimetric image analysis. In a rectangular sensor platform, a qualitative visualization of oxygen distribution over a wide area (60 mm x 90 mm) was demonstrated. Also, it was possible to establish polynomial calibration curves for quantitative oxygen analysis across a Y-junction channel (40 mm wide) sensor platform. Therefore, the LCD monitors and the color cameras exhibit a great potential as inexpensive colorimetric chemical instruments with unique features of large-area and high-throughput analysis.

**APPENDIX A.**  
**DETAILED PROCEDURE FOR OXYGEN SENSOR COCKTAIL**

For the oxygen sensor platform fabrication, a ruthenium (II) base oxygen sensing solution was prepared by mixing several additives with ruthenium (II). The entire procedure for preparation of the oxygen sensor cocktail is described in Table A.1.

Table A.1. Oxygen sensor cocktail preparation

<i>Sr. No.</i>	<i>Process</i>	<i>Equipment/Chemicals used</i>	<i>Procedure</i>
1	Dissolve ruthenium in solvent	Ruthenium (II) complex, toluene, glass bottle, electronic scale, stirring machine	- Dissolve 0.375 mg Ru(II) in 10 ml of toluene using a glass bottle covered with black material - Stirring : 30 minutes
2	Add an absorbent	Fumed silica particles electronic scale, stirring machine	- Add 0.6 g fumed silica into the glass bottle - Stirring : 24 hours
3	Preparation PDMS	Two-part silicone, vacuum chamber	- Mixed with 6.6 ml solution of 10:1 PDMS pre-polymer : curing agent - Placed in vacuum chamber : 30 minutes
4	Add silicone	Stirring machine	- Add 6.6 ml silicone in the glass bottle - Stirring : 30 minutes

**APPENDIX B.**  
**SENSOR PLATFORM PREPERATION**

Two different types of sensor platforms are prepared for this study. Each sensor platform consists of a pair of glass plates, rubber spacer, polyethylene tubing (inner diameter 1/8"). The bottom glass plate was coated with sensing material. The material information is presented in Table B.1 and entire sensor platform making procedure is presented in Table B.2. Fig. B.1 shows the real scale channel designs.

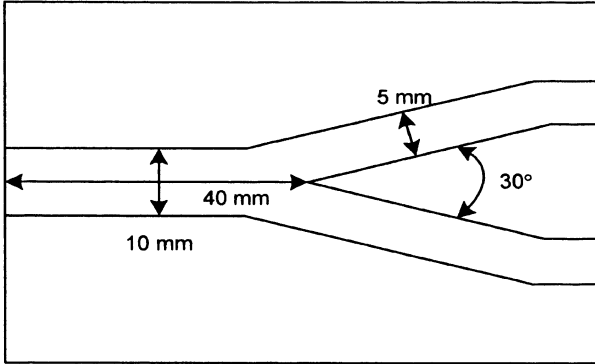
Table B.1. Material information

No.	Material	Dimension / number	Purpose
1	Glass plate I	75 mm x 50 mm x 1 mm 2 slides	- Y-junction type sensor platform back and front
2	Glass plate II	150 mm x 100 mm x 1 mm	- Meso-scale type sensor platform back and front
3	Rubber spacer	Thickness : 2 mm	- Channel wall
4	Tubing	Inner diameter : 1/8 inch	- inlet and outlet
5	Sponge filter	Thickness : 3 mm	- Meso-scale type sensor inner wall - reduce the gas pressure

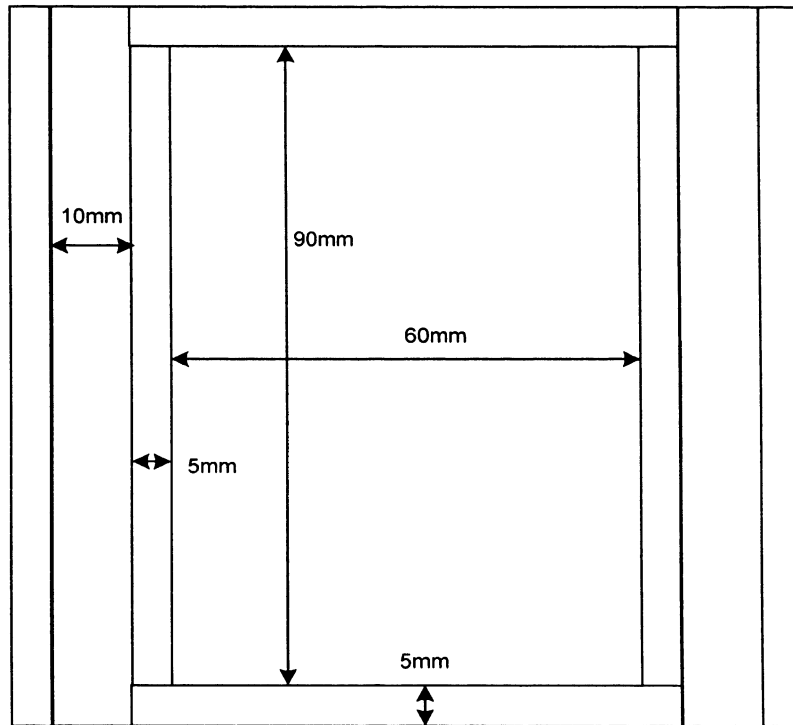
Table B.2. Photographing conditions for phosphorescent imaging

Sr. No.	Process	Equipment/Chemicals used	Procedure
1	Glass plate preparation	Glass plates, DI water, soap	- Wash the glass plates using soap
2	Spin coating	Oxygen sensor cocktail, pipette, spin coater (WS-400B-6NPP/LITE, Laurell Technologies)	- Spread sensor cocktail on entire glass plates using pipette - Spin at 300 rpm for 10 seconds - Baking at 65°C for 30 minutes
3	Channel design preparation	Printed channel design, rubber sheet, knife	- Placed printed channel design on the rubber sheet - Cut every line
4	Making sensor platform	Glass plates, rubber spacer, sponge filter, super glue, epoxy glue	- Apply super glue on the rubber spacers and place on bare glass plate on the rubber spacer - Flip over and remove rubber spacer inside channel area - Place sensor coated glass on the channel - Combined platform using epoxy glue - Attach the tubing

Fig. B.1 Sensor channel designs. (a) Y-junction channel, (b) Meso-scale rectangular fluidic sensor platform



(a)



(b)

**APPENDIX C.**  
**MATLAB CODE FOR IMAGE ANALYSIS**

Custom MATLAB code was written for image analysis. First, STEP-I was to pre-process all ten images obtained at a time to create a single average red intensity image to reduce noise. The purpose of second step, STEP-II, was to acquire a Stern-Volmer image (equivalent of  $I_0/I$  in the Stern-Volmer Eq.) to divide a nitrogen-saturated image (equivalent of  $I_0$ ) by other images at various conditions (equivalent of  $I$ ). In case of quantitative analysis to obtain calibration curves ( $I_0/I$  vs. oxygen percentages), STEP-III was executed by averaging Stern-Volmer value ( $I_0/I$ ) in each cropped region-of-interest (ROI) for calibration purpose. Overall sequence of two different m-files, one for qualitative imaging of oxygen distribution change with respect to time and the other for analysis of calibration images at different oxygen environment, are shown in Fig. C.1.

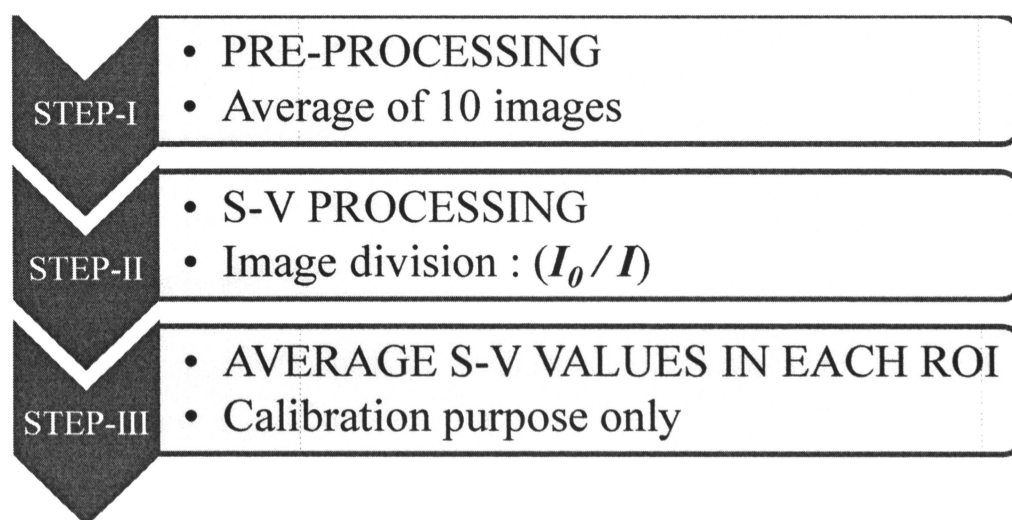


Fig. C.1 Image processing procedure

The MATLAB m-file for the qualitative imaging of oxygen distribution change with respect to time is as follows :

```
clear all; close all; clc;

% image read, summation, division process

% before : 0% oxygen concentration

im_base=double(imread('before1.jpg')); % change data format from uint8 to double
im_base=im_base(:,:,1); % red component extraction
im_add=double(imread('before2.jpg'));
im_add=im_add(:,:,1);
im_base=im_base+im_add; % image summation
im_add=double(imread('before3.jpg'));
im_add=im_add(:,:,1);
im_base=im_base+im_add;
im_add=double(imread('before4.jpg'));
im_add=im_add(:,:,1);
im_base=im_base+im_add;
im_add=double(imread('before5.jpg'));
im_add=im_add(:,:,1);
im_base=im_base+im_add;
im_add=double(imread('before6.jpg'));
im_add=im_add(:,:,1);
im_base=im_base+im_add;
im_add=double(imread('before7.jpg'));
im_add=im_add(:,:,1);
im_base=im_base+im_add;
im_add=double(imread('before8.jpg'));
im_add=im_add(:,:,1);
im_base=im_base+im_add;
im_add=double(imread('before9.jpg'));
im_add=im_add(:,:,1);
im_base=im_base+im_add;
im_add=double(imread('before10.jpg'));
im_add=im_add(:,:,1);
```

```
im_base=im_base+im_add;
clear im_add; im_base=im_base/10; % image division with total image number
```

```
% 10min after
```

```
im_10=double(imread('10min1.jpg'));
im_10=im_10(:,:,1);
im_10_add=double(imread('10min2.jpg'));
im_10_add=im_10_add(:,:,1);
im_10=im_10+im_10_add;
im_10_add=double(imread('10min3.jpg'));
im_10_add=im_10_add(:,:,1);
im_10=im_10+im_10_add;
im_10_add=double(imread('10min4.jpg'));
im_10_add=im_10_add(:,:,1);
im_10=im_10+im_10_add;
im_10_add=double(imread('10min5.jpg'));
im_10_add=im_10_add(:,:,1);
im_10=im_10+im_10_add;
im_10_add=double(imread('10min6.jpg'));
im_10_add=im_10_add(:,:,1);
im_10=im_10+im_10_add;
im_10_add=double(imread('10min7.jpg'));
im_10_add=im_10_add(:,:,1);
im_10=im_10+im_10_add;
im_10_add=double(imread('10min8.jpg'));
im_10_add=im_10_add(:,:,1);
im_10=im_10+im_10_add;
im_10_add=double(imread('10min9.jpg'));
im_10_add=im_10_add(:,:,1);
im_10=im_10+im_10_add;
im_10_add=double(imread('10min10.jpg'));
im_10_add=im_10_add(:,:,1);
im_10=im_10+im_10_add;
clear im_10_add; im_10=im_10/10;
```

```
% 20min after
```

```
im_20=double(imread('20min1.jpg'));
im_20=im_20(:,:,1);
im_20_add=double(imread('20min2.jpg'));
im_20_add=im_20_add(:,:,1);
im_20=im_20+im_20_add;
im_20_add=double(imread('20min3.jpg'));
im_20_add=im_20_add(:,:,1);
im_20=im_20+im_20_add;
im_20_add=double(imread('20min4.jpg'));
im_20_add=im_20_add(:,:,1);
im_20=im_20+im_20_add;
im_20_add=double(imread('20min5.jpg'));
im_20_add=im_20_add(:,:,1);
im_20=im_20+im_20_add;
im_20_add=double(imread('20min6.jpg'));
im_20_add=im_20_add(:,:,1);
im_20=im_20+im_20_add;
im_20_add=double(imread('20min7.jpg'));
im_20_add=im_20_add(:,:,1);
im_20=im_20+im_20_add;
im_20_add=double(imread('20min8.jpg'));
im_20_add=im_20_add(:,:,1);
im_20=im_20+im_20_add;
im_20_add=double(imread('20min9.jpg'));
im_20_add=im_20_add(:,:,1);
im_20=im_20+im_20_add;
im_20_add=double(imread('20min10.jpg'));
im_20_add=im_20_add(:,:,1);
im_20=im_20+im_20_add;
clear im_20_add; im_20=im_20/10;

% ROI coordinate check
red_ex=uint8(im_20);
imshow(red_ex); % image display

% entire channel area cropping
im_base=imcrop(im_base,[1295 995 2048 1072]);
```

```
im_10=imcrop(im_10,[1295 995 2048 1072]);
im_20=imcrop(im_20,[1295 995 2048 1072]);

% vertical line cropping
v1_base=imcrop(im_base,[738 373 29 299]);
MV1_base=mean(v1_base,2); % averaging horizontal 30 pixels
v1_20=imcrop(im_20,[738 373 29 299]);
MV1_20=mean(v1_20,2);

v2_base=imcrop(im_base,[394 373 29 299]);
MV2_base=mean(v2_base,2);
v2_20=imcrop(im_20,[394 373 29 299]);
MV2_20=mean(v2_20,2);

v3_base=imcrop(im_base,[59 382 29 299]);
MV3_base=mean(v3_base,2);
v3_20=imcrop(im_20,[59 382 29 299]);
MV3_20=mean(v3_20,2);

% plot original data of vertical lines
figure(100);
plot(MV1_base)
figure(200);
plot(MV1_20)
figure(300);
plot(MV2_base)
figure(400);
plot(MV2_20)
figure(500);
plot(MV3_base)
figure(600);
plot(MV3_20)

% image division with 0% oxygen image for Stern-Volmer type conversion
im_base_sv=im_base./im_base;
im_10_sv=im_base./im_10;
im_20_sv=im_base./im_20;
```

```
% cropping 20 minutes after image vertical data
im_20_v1_sv=imcrop(im_20_sv,[738 373 29 299]);
MV1=mean(im_20_v1_sv,2);

im_20_v2_sv=imcrop(im_20_sv,[394 373 29 299]);
MV2=mean(im_20_v2_sv,2);

im_20_v3_sv=imcrop(im_20_sv,[59 382 29 299]);
MV3=mean(im_20_v3_sv,2);

% display Stern-Volmer type data of vertical lines of 20 minutes after result.
figure(700);
plot(MV1)
figure(800);
plot(MV2)
figure(900);
plot(MV3)

% display entire channel 3-D image converted by Stern-Volmer type
figure(1000);
mesh(im_10_sv)
figure(1100);
mesh(im_20_sv)

% save results
save result_channel_2_17_reanal_pointchange.mat
```

The MATLAB m-file for the analysis of calibration images at different oxygen environment processing is as follows :

```
clear all; close all; clc

% Read original images

% 0% Oxygen concentration
im_base=double(imread('O01.jpg'));
im_base=im_base(:,:,1);
im_add=double(imread('O02.jpg'));
im_add=im_add(:,:,1);
im_base=im_base+im_add;
im_add=double(imread('O03.jpg'));
im_add=im_add(:,:,1);
im_base=im_base+im_add;
im_add=double(imread('O04.jpg'));
im_add=im_add(:,:,1);
im_base=im_base+im_add;
im_add=double(imread('O05.jpg'));
im_add=im_add(:,:,1);
im_base=im_base+im_add;
im_add=double(imread('O06.jpg'));
im_add=im_add(:,:,1);
im_base=im_base+im_add;
im_add=double(imread('O07.jpg'));
im_add=im_add(:,:,1);
im_base=im_base+im_add;
im_add=double(imread('O08.jpg'));
im_add=im_add(:,:,1);
im_base=im_base+im_add;
im_add=double(imread('O09.jpg'));
im_add=im_add(:,:,1);
im_base=im_base+im_add;
im_add=double(imread('O010.jpg'));
im_add=im_add(:,:,1);
im_O0=im_base+im_add;
```

```
clear im_add; clear im_base; im_O0=im_O0/10;
```

```
% 5% Oxygen concentration
```

```
im_5=double(imread('O51.jpg'));  
im_5=im_5(:,:,1);  
im_5_add=double(imread('O52.jpg'));  
im_5_add=im_5_add(:,:,1);  
im_5=im_5+im_5_add;  
im_5_add=double(imread('O53.jpg'));  
im_5_add=im_5_add(:,:,1);  
im_5=im_5+im_5_add;  
im_5_add=double(imread('O54.jpg'));  
im_5_add=im_5_add(:,:,1);  
im_5=im_5+im_5_add;  
im_5_add=double(imread('O55.jpg'));  
im_5_add=im_5_add(:,:,1);  
im_5=im_5+im_5_add;  
im_5_add=double(imread('O56.jpg'));  
im_5_add=im_5_add(:,:,1);  
im_5=im_5+im_5_add;  
im_5_add=double(imread('O57.jpg'));  
im_5_add=im_5_add(:,:,1);  
im_5=im_5+im_5_add;  
im_5_add=double(imread('O58.jpg'));  
im_5_add=im_5_add(:,:,1);  
im_5=im_5+im_5_add;  
im_5_add=double(imread('O59.jpg'));  
im_5_add=im_5_add(:,:,1);  
im_5=im_5+im_5_add;  
im_5_add=double(imread('O510.jpg'));  
im_5_add=im_5_add(:,:,1);  
im_O5=im_5+im_5_add;  
clear im_5_add; clear im_5; im_O5=im_O5/10;
```

```
% 10% Oxygen concentration
```

```
im_10=double(imread('O101.jpg'));
```

```
im_10=im_10(:,:,1);
im_10_add=double(imread('O102.jpg'));
im_10_add=im_10_add(:,:,1);
im_10=im_10+im_10_add;
im_10_add=double(imread('O103.jpg'));
im_10_add=im_10_add(:,:,1);
im_10=im_10+im_10_add;
im_10_add=double(imread('O104.jpg'));
im_10_add=im_10_add(:,:,1);
im_10=im_10+im_10_add;
im_10_add=double(imread('O105.jpg'));
im_10_add=im_10_add(:,:,1);
im_10=im_10+im_10_add;
im_10_add=double(imread('O106.jpg'));
im_10_add=im_10_add(:,:,1);
im_10=im_10+im_10_add;
im_10_add=double(imread('O107.jpg'));
im_10_add=im_10_add(:,:,1);
im_10=im_10+im_10_add;
im_10_add=double(imread('O108.jpg'));
im_10_add=im_10_add(:,:,1);
im_10=im_10+im_10_add;
im_10_add=double(imread('O109.jpg'));
im_10_add=im_10_add(:,:,1);
im_10=im_10+im_10_add;
im_10_add=double(imread('O1010.jpg'));
im_10_add=im_10_add(:,:,1);
im_O10=im_10+im_10_add;
clear im_10_add; clear im_10; im_O10=im_O10/10;
```

```
%% 15% Oxygen
```

```
im_15=double(imread('O151.jpg'));
im_15=im_15(:,:,1);
im_15_add=double(imread('O152.jpg'));
im_15_add=im_15_add(:,:,1);
im_15=im_15+im_15_add;
im_15_add=double(imread('O153.jpg'));
```

```
im_15_add=im_15_add(:,:,1);
im_15=im_15+im_15_add;
im_15_add=double(imread('O154.jpg'));
im_15_add=im_15_add(:,:,1);
im_15=im_15+im_15_add;
im_15_add=double(imread('O155.jpg'));
im_15_add=im_15_add(:,:,1);
im_15=im_15+im_15_add;
im_15_add=double(imread('O156.jpg'));
im_15_add=im_15_add(:,:,1);
im_15=im_15+im_15_add;
im_15_add=double(imread('O157.jpg'));
im_15_add=im_15_add(:,:,1);
im_15=im_15+im_15_add;
im_15_add=double(imread('O158.jpg'));
im_15_add=im_15_add(:,:,1);
im_15=im_15+im_15_add;
im_15_add=double(imread('O159.jpg'));
im_15_add=im_15_add(:,:,1);
im_15=im_15+im_15_add;
im_15_add=double(imread('O1510.jpg'));
im_15_add=im_15_add(:,:,1);
im_O15=im_15+im_15_add;
clear im_15_add; clear im_15; im_O15=im_O15/10;
```

```
% 20% Oxygen concentration
im_20=double(imread('O201.jpg'));
im_20=im_20(:,:,1);
im_20_add=double(imread('O202.jpg'));
im_20_add=im_20_add(:,:,1);
im_20=im_20+im_20_add;
im_20_add=double(imread('O203.jpg'));
im_20_add=im_20_add(:,:,1);
im_20=im_20+im_20_add;
im_20_add=double(imread('O204.jpg'));
im_20_add=im_20_add(:,:,1);
```

```
im_20=im_20+im_20_add;
im_20_add=double(imread('O205.jpg'));
im_20_add=im_20_add(:,:,1);
im_20=im_20+im_20_add;
im_20_add=double(imread('O206.jpg'));
im_20_add=im_20_add(:,:,1);
im_20=im_20+im_20_add;
im_20_add=double(imread('O207.jpg'));
im_20_add=im_20_add(:,:,1);
im_20=im_20+im_20_add;
im_20_add=double(imread('O208.jpg'));
im_20_add=im_20_add(:,:,1);
im_20=im_20+im_20_add;
im_20_add=double(imread('O209.jpg'));
im_20_add=im_20_add(:,:,1);
im_20=im_20+im_20_add;
im_20_add=double(imread('O2010.jpg'));
im_20_add=im_20_add(:,:,1);
im_O20=im_20+im_20_add;
clear im_20_add; clear im_20; im_O20=im_O20/10;

% ROI coordinate check
red_ex=uint8(im_O20);
imshow(red_ex); % image display

% crop point
mean_O0=mean(mean(imcrop(im_O0,[2746 1339 124 124])));
mean_O5=mean(mean(imcrop(im_O5,[2746 1339 124 124])));
mean_O10=mean(mean(imcrop(im_O10,[2746 1339 124 124])));
mean_O15=mean(mean(imcrop(im_O15,[2746 1339 124 124])));
mean_O20=mean(mean(imcrop(im_O20,[2746 1339 124 124])));

% absolute red intensity mean values
red_mean=[mean_O0,mean_O5,mean_O10,mean_O15,mean_O20];

% Stern-Volmer type conversion
```

```
SV_0=mean_O0/mean_O0;  
SV_5=mean_O0/mean_O5;  
SV_10=mean_O0/mean_O10;  
SV_15=mean_O0/mean_O15;  
SV_20=mean_O0/mean_O20;  
  
SV=[SV_0,SV_5,SV_10,SV_15,SV_20];  
  
% plot result  
X=[0 5 10 15 20];  
Figure(200);  
Plot(X SV)  
  
% save the result  
save result_calibration.mat
```

## VITA

Sanghan Park was born on September 1, 1975 in Daegu, Republic of Korea. He received his Bachelor of Engineering degree from Korea Military Academy , Republic of Korea, in Electrical Engineering in 1998. He is serving as an officer in the Army (May 1998 – present). He was awarded a scholarship from the Republic of Korea Army Headquarter to pursue his Master of Science in Electrical Engineering from Missouri University of Science and Technology (formerly University of Missouri-Rolla), and will graduate in July 2011.